



Measurement of exclusive $\rho(770)^0$ photoproduction in ultraperipheral pPb collisions at $\sqrt{s_{NN}} = 5.02$ TeV

CMS Collaboration*

CERN, 1211 Geneva 23, Switzerland

Received: 4 February 2019 / Accepted: 5 August 2019
© CERN for the benefit of the CMS collaboration 2019

Abstract Exclusive $\rho(770)^0$ photoproduction is measured for the first time in ultraperipheral pPb collisions at $\sqrt{s_{NN}} = 5.02$ TeV with the CMS detector. The cross section $\sigma(\gamma p \rightarrow \rho(770)^0 p)$ is 11.0 ± 1.4 (stat) ± 1.0 (syst) μb at $\langle W_{\gamma p} \rangle = 92.6$ GeV for photon–proton centre-of-mass energies $W_{\gamma p}$ between 29 and 213 GeV. The differential cross section $d\sigma/d|t|$ is measured in the interval $0.025 < |t| < 1$ GeV² as a function of $W_{\gamma p}$, where t is the squared four-momentum transfer at the proton vertex. The results are compared with previous measurements and theoretical predictions. The measured cross section $\sigma(\gamma p \rightarrow \rho(770)^0 p)$ has a power-law dependence on the photon–proton centre-of-mass, consistent with electron–proton collision measurements performed at HERA. The $W_{\gamma p}$ dependence of the exponential slope of the differential cross section $d\sigma/d|t|$ is also measured.

1 Introduction

Exclusive vector meson (VM) photoproduction, $\gamma p \rightarrow \text{VM}p$, has received renewed interest following recent studies of ultraperipheral collisions involving ions and protons at the CERN LHC [1, 2]. In such collisions, photon-induced interactions predominantly occur when the colliding hadrons are separated by a distance larger than the sum of their radii. In this case, one of the hadrons may emit a quasi-real photon that fluctuates into a quark-antiquark pair with the quantum numbers of the photon, which can then turn into a VM upon interacting with the other hadron. The interaction of the VM with the hadron proceeds via the exchange of the vacuum quantum numbers, the so-called pomeron exchange. Proton–lead (pPb) collisions are particularly interesting for studying photon–proton interactions [3, 4] because the large electric charge of the Pb nucleus strongly enhances photon emission. Also, in these events, one can determine the photon direction and hence the photon–proton centre-of-mass energy $W_{\gamma p}$ unambiguously. This advantage is not present in

symmetric colliding systems such as pp interactions. Exclusive VM photoproduction is interesting because the Fourier transform of the t distribution, with t being the squared four-momentum transfer at the proton vertex, is related to the two-dimensional spatial distribution of the struck partons in the plane transverse to the beam direction. Furthermore, some models suggest that the energy dependence of the integrated cross section and that of the t distribution may provide evidence of gluon saturation, as discussed in Refs. [5–10].

By using ultraperipheral pPb collisions at $\sqrt{s_{NN}} = 5.02$ TeV at the LHC, the ALICE Collaboration has measured the exclusive photoproduction of $J/\psi(1S)$ mesons in the centre-of-mass energy interval $20 < W_{\gamma p} < 700$ GeV [11, 12]. The LHCb Collaboration has studied exclusive $J/\psi(1S)$, $\psi(2S)$, and $Y(nS)$ photoproduction in pp collisions at $\sqrt{s} = 7$ and 8 TeV [13, 14]. Exclusive photoproduction of $\rho(770)^0$ mesons was first studied in fixed-target experiments at $W_{\gamma p}$ values up to 20 GeV [15, 16]. Experiments at the HERA electron–proton collider at DESY have studied this process at $W_{\gamma p}$ values ranging from 50 to 187 GeV, both with quasi-real photons and for photons with larger virtualities [17, 18]. The HERA data have provided clear experimental evidence for the transition from the soft to the hard diffractive regime [19, 20]. More recently, exclusive photoproduction of $\rho(770)^0$ mesons has been studied by the STAR Collaboration in ultraperipheral AuAu collisions at the BNL RHIC collider [21–23], and by the ALICE Collaboration in PbPb collisions [24]. The cross sections measured by the ALICE and STAR Collaborations in photon-nucleus interactions are 40% lower than both the prediction from the Glauber approach and the corresponding measurements in photon–proton interactions [24, 25]. However, the Glauber approach reproduces the measured cross sections well at lower energies. This is an indication that nuclei do not behave as a collection of independent nucleons at high energies. In the present analysis, exclusive photoproduction of $\rho(770)^0$ mesons in the $\pi^+ \pi^-$ decay channel in ultraperipheral pPb collisions at

* e-mail: cms-publication-committee-chair@cern.ch

$\sqrt{s_{\text{NN}}} = 5.02$ TeV is measured. The cross section is measured as a function of $W_{\gamma\text{p}}$ and t . In this paper $|t|$ is defined as the squared transverse momentum of the $\rho(770)^0$ meson, $|t| \approx p_{\text{T}}^2$.

This paper is organized as follows. Section 2 describes the experimental apparatus and Sect. 3 the data and simulated Monte Carlo samples. The event selection procedure is illustrated in Sect. 4. Section 5 discusses the background contributions and Sect. 6 the strategy used to extract the signal; the systematic uncertainties are summarized in Sect. 7. The total and differential cross sections are presented in Sect. 8. The results are summarized in Sect. 9.

2 The CMS detector

The central feature of the CMS apparatus is a superconducting solenoid of 6 m internal diameter, providing a magnetic field of 3.8 T. Within the solenoid volume are a silicon pixel and strip tracker, a lead tungsten crystal electromagnetic calorimeter (ECAL), and a brass and scintillator hadron calorimeter (HCAL), each composed of a barrel and two endcap sections. The silicon tracker measures charged particles within the range $|\eta| < 2.5$. It consists of 1440 silicon pixel and 15,148 silicon-strip detector modules and is located in the field of the superconducting solenoid. For non-isolated particles of $1 < p_{\text{T}} < 10$ GeV and $|\eta| < 1.4$, the track resolutions are typically 1.5% in p_{T} and 25–90 (45–150) μm in the transverse (longitudinal) direction [26].

The pseudorapidity coverage for the ECAL and HCAL detectors is $|\eta| < 3.0$. The ECAL provides coverage in the pseudorapidity range $|\eta| < 1.5$ in the barrel (EB) region and $1.5 < |\eta| < 3.0$ in the two endcap (EE) regions. The HCAL provides coverage for $|\eta| < 1.3$ in the barrel (HB) region and $1.3 < |\eta| < 3.0$ in the two endcap (HE) regions. The hadron forward (HF) calorimeters ($3.0 < |\eta| < 5.2$) complement the coverage provided by the barrel and endcap detectors. The zero-degree calorimeters (ZDCs) are two Čerenkov calorimeters composed of alternating layers of tungsten and quartz fibers that cover the region $|\eta| > 8.3$. Both the HF and ZDC detectors are divided into two halves, one covering positive pseudorapidities, the other negative, and referred to as HF+ and ZDC+ (and HF- and ZDC-), respectively. Another calorimeter, CASTOR, also a Čerenkov sampling calorimeter, consists of quartz and tungsten plates and is located only at negative pseudorapidities with coverage of $-6.6 < \eta < -5.2$.

A more detailed description of the CMS detector, together with the definition of the coordinate system used and the relevant kinematic variables, can be found in Ref. [27].

3 Data and Monte Carlo simulation

This analysis uses data from pPb collisions at $\sqrt{s_{\text{NN}}} = 5.02$ TeV collected with the CMS detector in February 2013. The beam energies are 4 TeV for the protons and 1.58 TeV per nucleon for the lead nuclei. The integrated luminosity is $\mathcal{L} = 7.4 \mu\text{b}^{-1}$ for the pPb data set (protons circulating in the negative z direction) and $\mathcal{L} = 9.6 \mu\text{b}^{-1}$ for the PbP data set (protons circulating in the positive z direction). Since the events are asymmetric in rapidity, the pPb and PbP samples are merged after changing the sign of the rapidity in the PbP sample.

The STARLIGHT (version 2.2.0) Monte Carlo (MC) event generator [28] is used to simulate exclusive $\rho(770)^0$ photoproduction followed by the $\rho(770)^0 \rightarrow \pi^+\pi^-$ decay. The STARLIGHT generator models two-photon and photon-hadron interactions at ultrarelativistic energies. Two processes contribute to the exclusive $\pi^+\pi^-$ channel: resonant $\rho(770)^0 \rightarrow \pi^+\pi^-$ production, and nonresonant $\pi^+\pi^-$ production, including the interference term. Both processes are generated in order to calculate the signal acceptance and efficiency, and to extract the corrected signal yield. STARLIGHT is also used to generate exclusive $\rho(1700)$ events. The pPb and PbP samples are produced separately. The events are passed through a detailed GEANT4 [29] simulation of the CMS detector in order to model the detector response, and are reconstructed with the same software used for the data.

4 Event selection

Table 1 presents the number of events after each selection requirement is applied. Events were selected online [30] by requiring the simultaneous presence of the two beams at the interaction point, as measured by the beam monitor timing system, in conjunction with at least one track in the pixel tracker. Offline, events are discarded if they have an energy deposit in any of the HF towers above the noise threshold of 3 GeV. Events are also required to have exactly two tracks that pass the selection criteria defined in Ref. [31], and to be associated with a single vertex located within 15 cm of the nominal interaction point along the beam direction. The pion mass is assigned to each track. In order to minimize the effect of the uncertainty in the low- p_{T} track efficiency, one of the tracks should have a p_{T} larger than 0.4 GeV, and the other larger than 0.2 GeV. Both tracks are selected in the interval $|\eta| < 2.0$. The rapidity of the $\pi^+\pi^-$ system is required to be in the interval $|y_{\pi^+\pi^-}| < 2.0$. To reject the photoproduction of $\rho(770)^0$ mesons from γPb interactions where the proton radiates a quasi-real photon, the p_{T} of the $\pi^+\pi^-$ system is required to be larger than 0.15 GeV (as discussed in Sect. 5).

Table 1 Integrated luminosity and number of events after each of the selection requirements for the two data samples. The leading tower is the tower with the largest energy deposition in the calorimeter

Selection	Number of selected events	
	pPb 7.4 μb^{-1}	Pbp 9.6 μb^{-1}
Integrated luminosity		
Leading HF tower < 3.0 GeV	52,508	66,278
Exactly two tracks	17,771	21,583
Track purity [31]	16,085	20,278
$ \eta_{\text{track}} < 2.0$,	12,707	16,037
$p_{\text{T}}^{\text{leading}} > 0.4 \text{ GeV}$, $p_{\text{T}}^{\text{subleading}} > 0.2 \text{ GeV}$	12,364	15,572
$ z_{\text{vertex}} < 15 \text{ cm}$	11,924	15,052
Leading HE tower < 1.95 GeV	11,563	14,643
CASTOR energy < 9 GeV	9405	–
ZDC ⁺ energy < 500 GeV	–	12,475
ZDC [–] energy < 2000 GeV	9099	–
Opposite-sign pairs	8507	11,553
Same-sign pairs	592	922

A sizable background contribution comes from proton dissociative events, $\gamma p \rightarrow \rho(770)^0 p^*$, where p^* indicates a low-mass hadronic state. In these events the scattered proton is excited and then dissociates. The $\rho(770)^0$ is measured in the central region, whereas the low-mass state usually escapes undetected. To suppress this contribution, events with activity above noise thresholds in the CASTOR, HE, HF, and ZDC detectors are rejected. The signal-to-noise ratio in ZDC⁺ is better than in ZDC[–] because of differences in radiation damage to the two detectors. For this reason, the ZDC energy thresholds shown in Table 1 are asymmetric. CASTOR is used for only the pPb sample because of its location, as discussed in Sect. 2. The final selection requires the two tracks to have opposite charges. A total of 20,060 opposite-sign pair events and 1514 same-sign pair events are selected in this analysis.

5 Background

The main background sources are listed below.

- *Nonresonant $\pi^+\pi^-$ production.* This contributes mainly through an interference term. It is included when fitting the invariant mass distribution, as discussed in Sect. 6.
- *Exclusive photoproduction of $\omega(783)$ and $\phi(1020)$ mesons.* Contamination from the decay $\phi(1020) \rightarrow K^+K^-$ is removed by assigning the kaon mass to the tracks and rejecting events with invariant mass values of the K^+K^- system larger than 1.04 GeV. In addition, contamination is expected from the $\omega(783) \rightarrow \pi^+\pi^-\pi^0$ and $\phi(1020) \rightarrow \pi^+\pi^-\pi^0$ decays when the photons from the π^0 decay are undetected. Although the $\pi^+\pi^-$ invariant

mass in these cases is mostly below the $\rho(770)$ mass, the rate of $\omega(783)$ and $\phi(1020)$ meson production increases with $|t|$. As observed in this analysis and at HERA [32], undetected photons lead to an overestimate of the p_{T} imbalance in the event, mimicking large $|t|$ events. Since these processes cannot be modeled by STARLIGHT, their contribution is estimated from the fits of the unfolded invariant mass distributions described in Sect. 6. The $\omega(783) \rightarrow \pi^+\pi^-\pi^0$ amplitude is small, but is clearly visible through its interference with the $\rho(770)^0$, which produces the small kink in the invariant mass spectrum near 800 MeV. This contribution is included in the invariant mass fit, as discussed in Sect. 6.

- *Exclusive photoproduction of $\rho(1700)$ mesons.*¹ The $\rho(1700)$ decays mostly into a $\rho(770)^0$ meson and a pion pair, leading to final states with four charged pions, or with two charged pions and two neutral pions. The $\rho(1700) \rightarrow \pi^+\pi^-\pi^+\pi^-$ decay may also result in opposite-sign events when only two opposite-sign pions are detected because of the limited rapidity coverage of the detector. Such events will appear to have a p_{T} imbalance, causing them to be incorrectly identified as large $|t|$ $\rho(770)^0$ events, thereby resulting in

¹ The data on the photoproduction of excited $\rho(1700)$ states in the four-pion decay channel are currently limited. A resonance structure with a broad invariant mass distribution around 1600 MeV is reported in the literature. According to the Particle Data Group this resonance has two components: the $\rho(1450)$ and the $\rho(1700)$ [33]. The nature of these states is still under investigation. Recently, the STAR Collaboration reported a measurement of exclusive photoproduction of four charged pions [34]. Their data are consistent with the $\rho(1700)$ assuming that the peak is dominated by spin states with $J^{PC} = 1^{--}$. In order to reproduce these data, STARLIGHT assumes a single resonance with a mass of 1540 MeV and a width of 570 MeV [28]. In the present paper, this state is referred to as $\rho(1700)$.

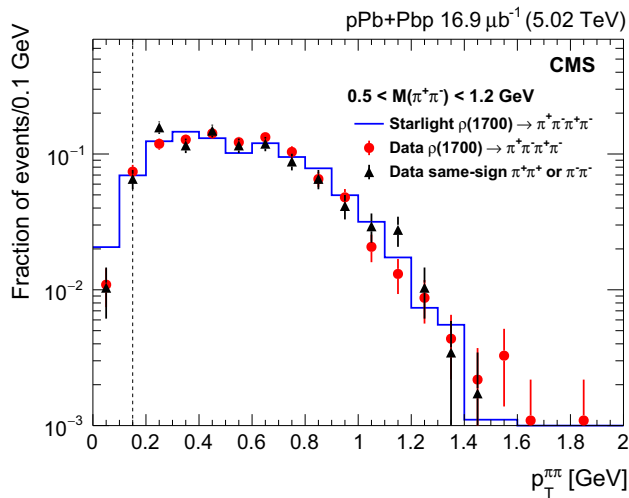


Fig. 1 Comparison between the $p_T^{\pi^+\pi^-}$ distributions of the reconstructed $\rho(1700)$ mesons in the data (full symbols) and the STARLIGHT simulation (histogram) when only two oppositely charged pions are selected. The triangles correspond to same-sign two-track events (either $\pi^+\pi^+$ or $\pi^-\pi^-$) in the data; they mostly come from $\rho(1700)$ decays with two undetected pions. The integrals of all three distributions are normalized to unity. Vertical bars correspond to the statistical uncertainties. The region to the left of the dashed vertical line is not included in the analysis (see Sect. 5 for details)

a distortion of the $|t|$ distribution. To validate the use of STARLIGHT for $\rho(1700)$ photoproduction, exclusive $\pi^+\pi^-\pi^+\pi^-$ events are selected in the data. The data sample and the STARLIGHT simulation for $\rho(1700)$ exclusive photoproduction are studied by applying the same selection criteria as for the $\rho(770)^0$, except that on the number of tracks. Figure 1 shows a comparison of the $p_T^{\pi^+\pi^-}$ distributions of the reconstructed $\rho(1700)$ mesons in the four pion event samples obtained from the data and the STARLIGHT simulation. All combinations of two oppositely charged pions are plotted in Fig. 1 if they have an invariant mass $0.5 < M_{\pi^+\pi^-} < 1.2$ GeV. In addition, the distribution of the same-sign events in the data is shown; they come mostly from $\rho(1700)$ decays with two missing pions. Figure 1 shows that the data and the STARLIGHT results are in agreement, lending confidence to the performance of this generator. These distributions provide a template for the $p_T^{\pi^+\pi^-}$ distribution of the $\rho(1700)$ background used to estimate its contribution, as described in Sect. 6.

- *Proton dissociative $\rho(770)^0$ photoproduction.* This contribution is suppressed by rejecting events with activity in the CASTOR, HE, HF, and ZDC detectors. In order to determine the residual contribution, a sample of dissociative events is selected by requiring activity in at least one of the forward detectors (CASTOR, HF, or ZDC).

This sample provides a template for the $p_T^{\pi^+\pi^-}$ distribution of the dissociative events, under the assumption that the $p_T^{\pi^+\pi^-}$ distribution is independent of the mass of the dissociative system (the more forward the detector, the smaller the masses to which it is sensitive). Finally, this template is used to estimate the remaining dissociative background contributions, as discussed in Sect. 6.

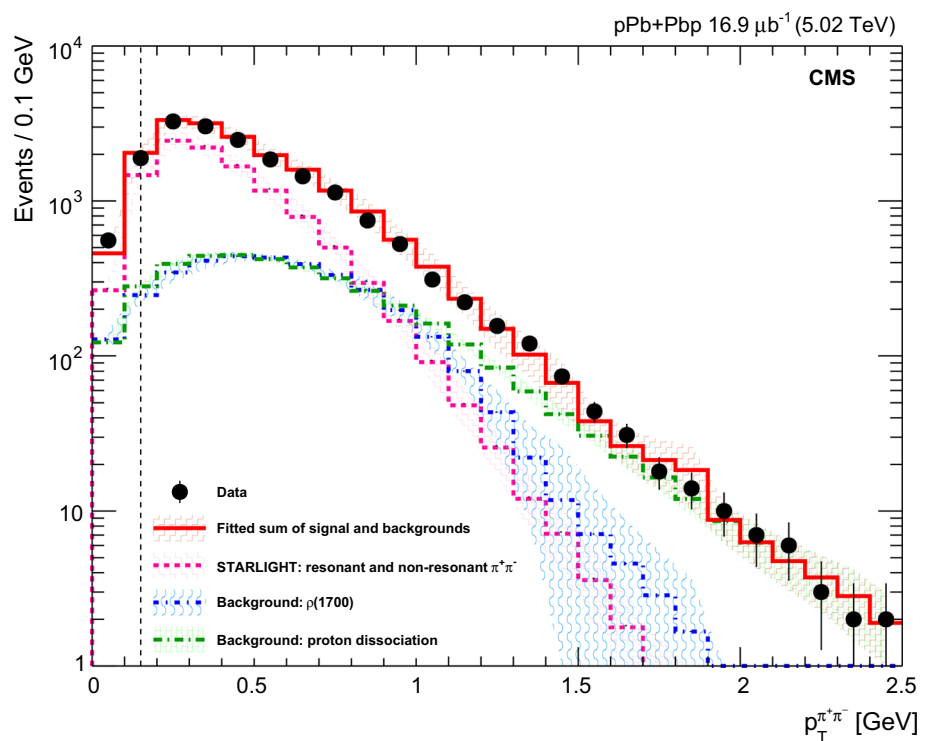
- *Double pomeron exchange processes and photoproduction processes from γ Pb interactions.* Since the strong force has short range, only the nucleons on the surface of the nucleus may contribute to double pomeron exchange interactions; the corresponding cross section is therefore negligible [35]. For coherent processes in γ Pb interactions, the size of the lead ion restricts the mean p_T of the VM to be about 60 MeV, corresponding to a de Broglie wavelength of the order of the nucleus size. Taking into account the detector resolution, all coherent $\rho(770)^0$ events have p_T less than 0.15 GeV. Thus, events from γ Pb interactions contribute to the lowest $|t|$ region, which is not included in this analysis.

6 Signal extraction

The extraction of the signal is carried out in two steps. First, the proton dissociative and the $\rho(1700)$ contributions are estimated by performing a fit to the data as a function of $p_T^{\pi^+\pi^-}$. This method relies on the fact that exclusive $\rho(770)^0$ events contribute mainly to the low- $p_T^{\pi^+\pi^-}$ region ($p_T^{\pi^+\pi^-} < 0.7$ GeV), whereas nonexclusive events dominate the high- $p_T^{\pi^+\pi^-}$ region ($p_T^{\pi^+\pi^-} > 1.2$ GeV), and the $\rho(1700)$ contribution is mostly at intermediate $p_T^{\pi^+\pi^-}$ values ($0.7 < p_T^{\pi^+\pi^-} < 1.2$ GeV). This makes the identification of the proton dissociative and the $\rho(1700)$ contributions robust. Second, the yield of exclusive $\rho(770)^0$ candidates is extracted by performing a fit to the unfolded invariant mass distribution. Since the events from exclusive $\rho(1700)$ production have a different invariant mass distribution from the signal events, they are subtracted before correcting the data for acceptance and efficiency. Conversely, the proton dissociative background has the same invariant mass and angular distributions as the signal, and its effect is corrected after unfolding by scaling the observed yields according to the fit performed in the first step.

To extract the normalizations of the proton dissociative and the $\rho(1700)$ backgrounds, an unbinned maximum likelihood fit is performed to the data as a function of $p_T^{\pi^+\pi^-}$ in the rapidity interval $|y_{\pi^+\pi^-}| < 2$. The sum of the following distributions is fitted to the data at the reconstructed level: the

Fig. 2 The measured distribution of the reconstructed $\pi^+\pi^-$ transverse momentum (full circles) together with the fitted sum of signal and backgrounds described in the text (red solid histogram). The STARLIGHT direct $\pi^+\pi^-$ contribution (pink dotted histogram), the $\rho(1700)$ background (blue dotted-short-dashed histogram), and the proton-dissociative contribution (green dotted-long-dashed histogram) are also shown. The shaded areas represent the systematic uncertainties. The region to the left of the dashed vertical line is not included in the analysis (see Sect. 5 for details)



signal distribution and the $\pi^+\pi^-$ continuum, as simulated by STARLIGHT, the distribution of the proton dissociative background, which is extracted from the data control sample, and the $\rho(1700)$ fitting template, which is simulated using STARLIGHT. The normalization of each of these components is determined from the fit. The signal $p_T^{\pi^+\pi^-}$ distribution generated by STARLIGHT is reweighted to describe the data using the theory-inspired expression $e^{-b|t|}$ [15]. The initial b value of STARLIGHT is 12 GeV^{-2} and the reweighted b is $13.1^{+0.4}_{-0.3} \text{ (stat) GeV}^{-2}$.

The result of the fit of the $p_T^{\pi^+\pi^-}$ distributions is shown in Fig. 2, including the systematic uncertainties associated with the fitting procedure that are discussed in Sect. 7. The resulting residual proton-dissociative and $\rho(1700)$ contributions, over the whole rapidity interval, are $18 \pm 2\%$ (stat) and $20 \pm 2\%$ (stat), respectively. Similar fractions of proton dissociative and $\rho(1700)$ contributions are obtained in the four rapidity intervals used in the differential cross section measurement as a function of rapidity. This is consistent with the small energy dependence of these processes in the energy range of this analysis. As seen in Fig. 2, the signal and both background contributions are of the same order of magnitude around $p_T^{\pi^+\pi^-} = 1 \text{ GeV}$, corresponding to a signal-to-background ratio of about 30%. For this reason, only the region $|t| < 1 \text{ GeV}^2$ is used in this measurement.

The $\rho(1700)$ background is subtracted in bins of invariant mass using the normalization obtained from the $p_T^{\pi^+\pi^-}$ fitting

templates. The invariant mass distribution is then unfolded using the iterative D’Agostini method [36], which is regularized by four iterations. In particular, the Bayesian iterative unfolding technique is used, as implemented in the ROOUNFOLD package [37]. This procedure leads to corrections for experimental effects including possible data migration between bins. The response matrix is obtained from STARLIGHT. The average of the combined acceptance and efficiency is 0.13 and is almost independent of both p_T and η , whereas it is sensitive to the invariant mass.

The invariant mass shape of the $\rho(770)^0$ in photoproduction deviates from that of a pure Breit–Wigner resonance [38]. Several parameterizations of the shape exist. One of the most often used is the Söding formula [39], where a continuum amplitude B is added to a Breit–Wigner distribution. Following the recent results by the STAR Collaboration [23] and the earlier ones by the DESY-MIT Collaboration [40], a further relativistic Breit–Wigner component is added to account for $\omega(783)$ photoproduction, followed by the decay $\omega(783) \rightarrow \pi^+\pi^-$. This leads to the following fitting function:

$$\frac{dN_{\pi^+\pi^-}}{dM_{\pi^+\pi^-}} = \left| A \frac{\sqrt{M_{\pi^+\pi^-} - M_{\rho(770)}} \Gamma_{\rho(770)}}{M_{\pi^+\pi^-}^2 - M_{\rho(770)}^2 + i M_{\rho(770)} \Gamma_{\rho(770)}} + B + C e^{i\phi_\omega} \frac{\sqrt{M_{\pi^+\pi^-} - M_{\omega(783)}} \Gamma_{\omega(783) \rightarrow \pi\pi}}{M_{\pi^+\pi^-}^2 - M_{\omega(783)}^2 + i M_{\omega(783)} \Gamma_{\omega(783)}} \right|^2.$$

Here A is the amplitude of the $\rho(770)^0$ Breit–Wigner function, B is the amplitude of the direct nonresonant $\pi^+\pi^-$ production, C is the amplitude of the $\omega(783)$ contribution, and the mass-dependent widths are given by

$$\Gamma_{\rho(770)} = \Gamma_0 \frac{M_{\rho(770)}^0}{M_{\pi^+\pi^-}} \left[\frac{M_{\pi^+\pi^-}^2 - 4m_{\pi^\pm}^2}{M_{\rho(770)}^0 - 4m_{\pi^\pm}^2} \right]^{\frac{3}{2}},$$

and

$$\Gamma_{\omega(783)} = \Gamma_0 \frac{M_{\omega(783)}}{M_{\pi^+\pi^-}} \left[\frac{M_{\pi^+\pi^-}^2 - 9m_{\pi^\pm}^2}{M_{\omega(783)} - 9m_{\pi^\pm}^2} \right]^{\frac{3}{2}},$$

where Γ_0 is the pole width for each meson and m_{π^\pm} is the charged pion mass. Since the branching fraction (\mathcal{B}) for $\omega(783) \rightarrow \pi^+\pi^-$ is small, only the first order term in the $\omega(783) - \rho(770)^0$ mass mixing theory is considered [40], leading to

$$\Gamma_{\omega(783) \rightarrow \pi\pi} = \mathcal{B}(\omega(783) \rightarrow \pi\pi) \Gamma_0 \frac{M_{\omega(783)}}{M_{\pi^+\pi^-}} \left[\frac{M_{\pi^+\pi^-}^2 - 4m_{\pi^\pm}^2}{M_{\omega(783)} - 4m_{\pi^\pm}^2} \right]^{\frac{3}{2}},$$

with $\mathcal{B}(\omega(783) \rightarrow \pi\pi) = 0.0153^{+0.0011}_{-0.0013}$ [33]. The H1 and ZEUS measurements did not include the $\omega(783) - \rho(770)^0$ interference component, although the ZEUS data seem to indicate its effect in the mass spectrum near 800 MeV [17].

Figure 3 shows the fit of the unfolded distribution with the modified Söding model. A least squares fit is performed for the interval $0.6 < M_{\pi^+\pi^-} < 1.1$ GeV, with the quantities $M_{\rho(770)}^0$, $M_{\omega(783)}$, $\Gamma_{\rho(770)}^0$, $\Gamma_{\omega(783)}$, A , B , C , and $\phi_{\omega(783)}$ treated as free parameters. This model includes the interference between resonant $\rho(770)^0$ and direct $\pi^+\pi^-$ production, as well as between $\rho(770)^0$ and $\omega(783)$ production. To correct for the $\omega(783)$ reflection in the $\pi^+\pi^-$ mass spectrum, a Gaussian function peaking around 500 MeV [18] is added as a further component of the invariant mass fit. This is only visible at high $|t|$ values, as shown in Fig. 4. The fit yields $M_{\rho(770)}^0 = 773 \pm 1$ (stat) MeV and $\Gamma_{\rho(770)}^0 = 148 \pm 3$ (stat) MeV, and $M_{\omega(783)} = 776 \pm 2$ (stat) MeV, consistent with the world average values [33]. The fitted value of the $\omega(783)$ width, $\Gamma_{\omega(783)} = 30 \pm 5$ (stat) MeV, is instead larger than the world average because of the detector resolution.

The $|B/A|$ and C/A fractions are also determined; they measure the ratios of the nonresonant and $\omega(783)$ contributions to the resonant $\rho(770)^0$ production, respectively. Since the ZEUS Collaboration found that $|B/A|$ decreases as $|t|$ increases, the fit is repeated for $|t| < 0.5$ GeV² resulting in 0.50 ± 0.06 (stat) GeV^{-1/2}. For this kinematic region H1 measured $|B/A| = 0.57 \pm 0.09$ (stat) GeV^{-1/2} and

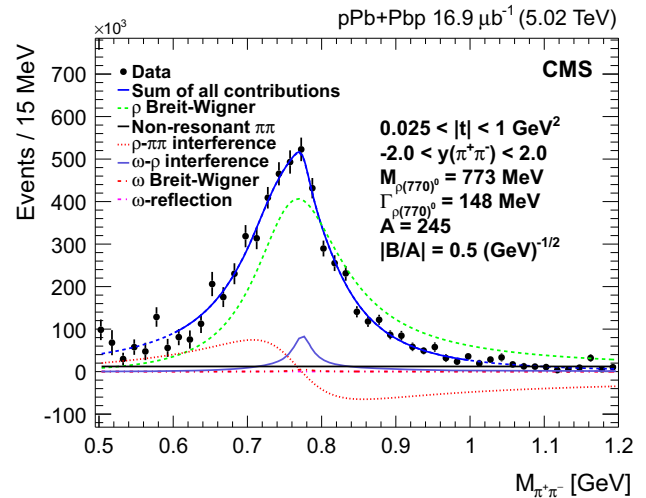


Fig. 3 Unfolded $\pi^+\pi^-$ invariant mass distribution in the pion pair rapidity interval $|y_{\pi^+\pi^-}| < 2.0$ (full circles) fitted with the modified Söding model. The results of the fit are also given (see text for details). The green dashed line indicates resonant $\rho(770)^0$ production, the red dotted line the interference term, the black dash-dotted line the non-resonant contribution, the dark blue dashed line the interference between $\rho(770)^0$ and $\omega(783)$, and the blue solid line represents the sum of all these contributions

ZEUS $|B/A| = 0.70 \pm 0.04$ (stat) GeV^{-1/2}. If the fit is repeated without the $\omega(783) - \rho(770)^0$ interference component, the result for $|B/A|$ changes by less than its statistical uncertainty. The measured ratio of the $\omega(783)$ to $\rho(770)^0$ amplitudes is $C/A = 0.40 \pm 0.06$ (stat), consistent with the prediction of STARLIGHT, $C/A = 0.32$, and the measurements of the STAR [23] and the DESY-MIT [40] experiments, which report $C/A = 0.36 \pm 0.03$ (stat) and $C/A = 0.36 \pm 0.04$ (stat), respectively. The present fit gives a nonzero $\omega(783)$ phase angle, $\phi_{\omega(783)} = 1.8 \pm 0.3$ (stat), also in agreement with the previous measurements [23, 40].

Additionally, the fit is performed in $|t|$ and y bins as shown in Fig. 4. To ensure fit stability, the $M_{\rho(770)}^0$, $M_{\omega(783)}$, $\Gamma_{\rho(770)}^0$, $\Gamma_{\omega(783)}$, $\phi_{\omega(783)}$ and $|C/A|$ parameters are fixed to the values obtained for the full rapidity interval. The $\omega(783) \rightarrow \pi^+\pi^-\pi^0$ contribution increases with $|t|$, as reported by the H1 Collaboration [18] and as seen in Fig. 4. The $|B/A|$ ratio is found to be independent of $W_{\gamma p}$ and decreases with $|t|$, in agreement with results reported by ZEUS [17].

7 Systematic uncertainties

The following sources of systematic uncertainty are considered.

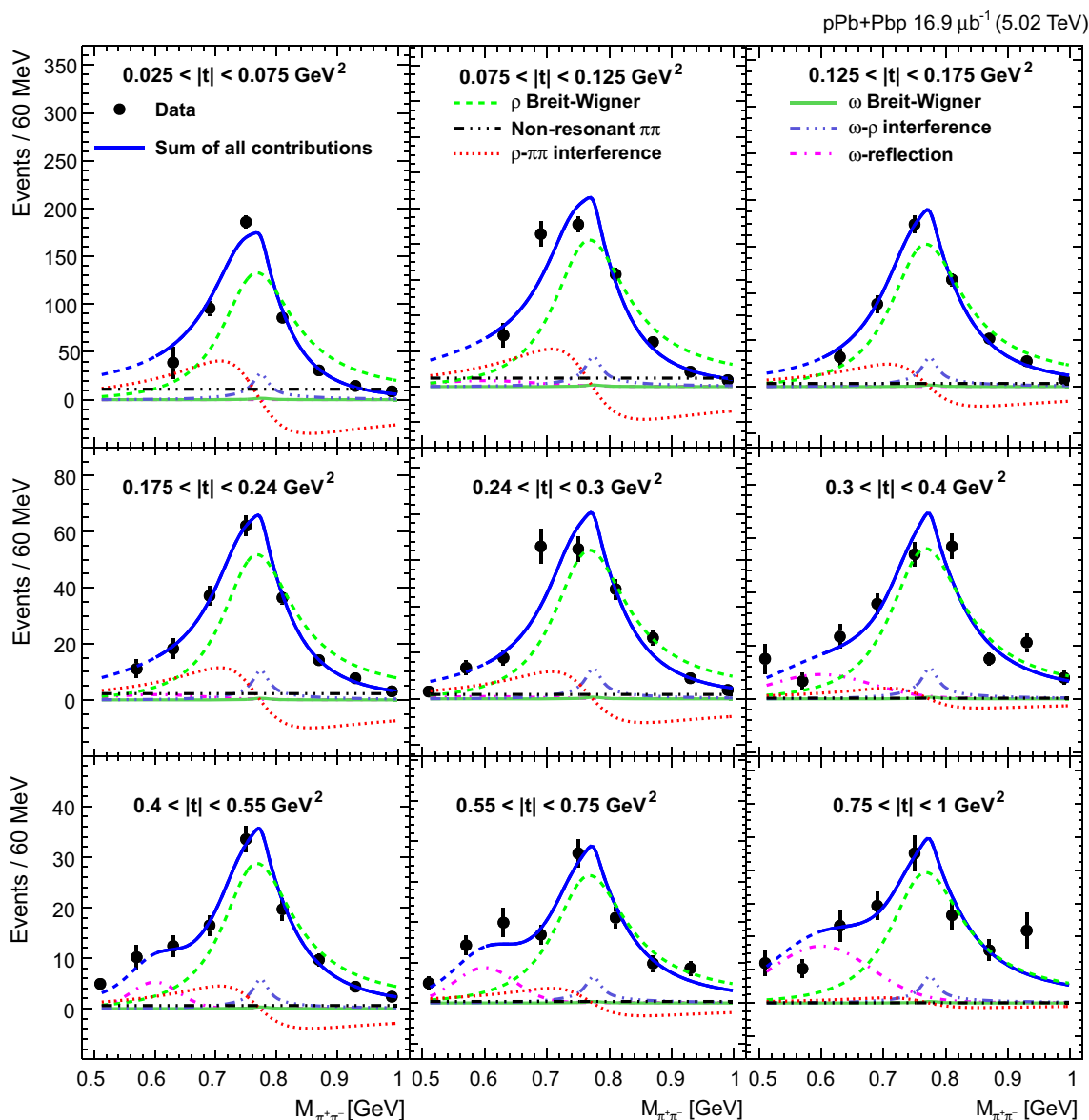


Fig. 4 Unfolded $\pi^+\pi^-$ invariant mass distributions in the pion pair rapidity interval $|y_{\pi^+\pi^-}| < 2.0$ (full circles) fitted with the Söding model in different $|t|$ bins. The green dashed lines indicate resonant $\rho(770)^0$ production, the red dotted lines the interference term, the magenta dash-dotted lines correspond to the background from

$\omega(783) \rightarrow \pi^0\pi^+\pi^-$, the black dash-dotted lines to the nonresonant contribution, the dark blue dashed line to the interference between $\rho(770)^0$ and $\omega(783)$, and the blue solid lines represent the sum of all these contributions

Integrated luminosity determination: The uncertainty in the integrated luminosity is 4% for both the pPb and Pbp samples [41].

Track reconstruction: The contribution of the tracking efficiency to the systematic uncertainty is studied with the method described in Ref. [26], where the ratio of yields of neutral charm mesons decaying to two-body and four-body final states is compared with data and simulation for pion momenta above 300 MeV. The accuracy of the detector sim-

ulation to reproduce the single-pion tracking efficiency is 3.9%. For the present measurement, this yields a 7.8% uncertainty.

Unfolding: The uncertainty associated with the unfolding procedure is determined by modifying the number of iterations used for the Bayesian unfolding from the nominal value of 4 to 3 and 5. The resulting uncertainty is smaller than that found when changing the model for building the response matrix. The latter is estimated by comparing two different

STARLIGHT samples: resonant $\rho(770)^0$ meson production, and combined resonant and nonresonant $\pi^+\pi^-$ production. The resulting effect on the integrated cross section is 3%.

Uncertainty in the photon flux: The uncertainty in the photon flux is 9% for the high- $W_{\gamma p}$ data point and 2% at low $W_{\gamma p}$, as discussed in Ref. [11]. The flux is computed in impact parameter space, convolved with the probability of no hadronic interactions. The radius of the lead nucleus is varied by the nuclear skin thickness (± 0.5 fm). In addition, in the calculation of the photon flux, the $\rho(770)^0$ pole mass in Eq. (1) is replaced by the reconstructed $\pi^+\pi^-$ mass on an event-by-event basis. The effect of this variation is negligible.

Calorimeter exclusivity: The uncertainty related to the exclusivity requirements is evaluated by varying the calorimeter energy thresholds. Increasing (or decreasing) the energy scale of the HF calorimeter towers by 5% results in a 1.0% variation of the exclusive $\pi^+\pi^-$ yields. The CASTOR energy scale is varied by 17% [42], resulting in a difference of 1% in the extracted $\rho(770)^0$ yield. The variations of the energy thresholds for HE and ZDC within their respective energy scale uncertainties have a negligible effect.

Background estimation: The uncertainty in the $\rho(1700)$ subtraction is evaluated by varying the normalization of the $\rho(1700)$ contribution by 20% with respect to that obtained from the fit shown in Fig. 2. As mentioned in Sect. 5, the proton dissociative background template is obtained by requiring a signal in at least one of the forward detectors: HF, CASTOR, or ZDC. To calculate the systematic uncertainty related to the estimation of this background, the analysis is repeated five times and each time alternative combinations of forward detectors are used to obtain the proton dissociative template. The following variations are studied: (i) HF alone; (ii) CASTOR alone; (iii) ZDC alone; (iv) HF or CASTOR; (v) HF or ZDC. For each of these combinations the proton dissociative contributions are obtained in each $|t|$ and rapidity bin. The maximum deviations from the nominal results are taken as conservative estimates of the systematic uncertainty. The resulting effect on the integrated exclusive $\rho(770)^0$ photoproduction cross section is smaller than 10%.

Model dependence: In order to assess the uncertainty due to the model used to fit the invariant mass distribution, the Ross–Stodolsky model [43] is used instead of the Söding model. The resulting cross section changes by up to 8%, depending on the rapidity and $|t|$ interval studied. Another contribution to the model dependence uncertainty comes from the reweighting procedure of the STARLIGHT MC described in Sect. 6. This uncertainty is evaluated by varying the reweighting parameter b within its uncertainty; it is found to increase as a function of $|t|$, and reaches 32% for the highest $|t|$ bin. The second contribution turns out to be dominant for all the rapidity and $|t|$ intervals studied. The uncertainty in

the extrapolation to the region $|t| < 0.025$ GeV² is model dependent. We estimated this uncertainty by studying different fitting functions to the differential cross section measurements. In particular, we studied a dipole form [28], a pure exponential e^{-bt} , and a modified exponential e^{-bt+ct^2} . The difference between the two most extreme extrapolated values is used as an estimate of the model dependence uncertainty.

The values of the systematic uncertainties for all $y_{\pi^+\pi^-}$ and $|t|$ intervals are summarized in Table 2. The systematic uncertainties are added in quadrature for the integrated photoproduction cross section. For the differential cross section results, the systematic uncertainties in Table 2 are treated as correlated between bins.

8 Results

The differential cross section for exclusive photoproduction of $\rho(770)^0$ mesons is given by

$$\frac{d\sigma}{dy} = \frac{N_{\rho(770)^0}^{\text{exc}}}{\mathcal{B}(\rho(770)^0 \rightarrow \pi^+\pi^-)L\Delta y},$$

where $N_{\rho(770)^0}^{\text{exc}}$ is the corrected number of exclusive $\rho(770)^0$ events obtained from the fits described in Sect. 6 by integrating the resonant component in the interval $0.28 < M_{\rho(770)^0} < 1.50$ GeV ($2M_{\pi^\pm} < M_{\rho(770)^0} < M_{\rho(770)^0} + 5\Gamma_{\rho(770)^0}$); \mathcal{B} is the branching fraction, which equals about 0.99 for the $\rho(770)^0 \rightarrow \pi^+\pi^-$ decay [33], Δy is the rapidity interval, and L is the integrated luminosity of the data sample. The cross section $d\sigma/dy(\text{pPb} \rightarrow \text{pPb}\rho(770)^0)$ is related to the photon–proton cross section, $\sigma(\gamma p \rightarrow \rho(770)^0 p) \equiv \sigma(W_{\gamma p})$, through the photon flux, dn/dk :

$$\frac{d\sigma}{dy}(\text{pPb} \rightarrow \text{pPb}\rho(770)^0) = k \frac{dn}{dk} \sigma(\gamma p \rightarrow \rho(770)^0 p).$$

Here, k is the photon energy, which is determined from the $\rho(770)^0$ mass and rapidity, according to the formula

$$k = (1/2)M_{\rho(770)^0} \exp(-y_{\rho(770)^0}). \quad (1)$$

The average photon flux and the average centre-of-mass energy ($\langle W_{\gamma p} \rangle$) values in each rapidity interval are calculated using STARLIGHT.

The unfolded invariant mass distribution is studied in different $|t|$ bins, and the extraction of the $\rho(770)^0$ photoproduction cross section is performed in each bin. In order to compare with the HERA results, the p_T -related measurements are presented in terms of $|t|$, which is approximated as $|t| \approx (p_T^{\pi^+\pi^-})^2$. Figure 5 shows the differential cross sections as a function of $|t|$, together with the unweighted STARLIGHT prediction, whose slope parameter is independent

Table 2 Summary of the systematic uncertainties in the $\rho(770)^0$ photoproduction cross section. The numbers are given in percent. The total uncertainty is calculated by adding the individual uncertainties in quadrature

$y_{\pi^+\pi^-}$ interval	(-2.0, 2.0)	(-2.0, -1.2)	(-1.2, 0.0)	(0.0, 1.2)	(1.2, 2.0)
Integrated luminosity	4.0	4.0	4.0	4.0	4.0
Track reconstruction	7.8	7.8	7.8	7.8	7.8
Unfolding	3.0	3.0	3.0	3.0	3.0
Photon flux calculation	5.0	2.0	4.0	6.0	9.0
Calorimeter exclusivity	1.4	1.4	1.4	1.4	1.4
Proton dissociation					
$ t [\text{GeV}^2]$					
0.025–1.000	2.3	1.6	2.3	3.6	3.9
0.025–0.075	2.3	1.6	2.3	3.6	3.9
0.075–0.120	1.9	1.5	1.8	2.9	3.2
0.12–0.17	2.3	1.7	2.1	3.3	3.7
0.17–0.24	3.0	2.2	2.7	4.0	4.9
0.24–0.30	3.9	2.5	3.4	5.5	6.8
0.3–0.4	5.2	3.7	4.6	7.1	9.2
0.40–0.55	7.1	5.8	6.5	9.8	13.0
0.55–0.75	10.0	9.7	9.0	14.0	19.0
0.75–1.00	14.0	19.0	11.0	22.0	28.0
$\rho(1700)$ background					
$ t [\text{GeV}^2]$					
0.025–1.000	4.3	13.0	1.9	7.1	2.0
0.025–0.075	4.3	13.0	1.9	7.1	2.0
0.075–0.120	4.8	1.3	2.0	2.0	7.4
0.12–0.17	5.6	2.9	2.7	4.5	5.6
0.17–0.24	5.8	3.6	5.9	3.2	4.9
0.24–0.30	3.8	4.4	6.6	5.8	16.0
0.3–0.4	6.5	14.0	7.3	11.0	17.0
0.40–0.55	9.1	19.0	21.0	9.7	14.0
0.55–0.75	35.0	37.0	13.0	20.0	55.0
0.75–1.00	46.0	56.0	19.0	39.0	32.0
Model dependence					
$ t [\text{GeV}^2]$					
0.025–1.000	5.1	5.1	5.1	5.1	5.1
0.025–0.075	5.1	5.1	5.1	5.1	5.1
0.075–0.120	5.5	5.5	5.5	5.5	5.5
0.12–0.17	6.6	6.6	6.6	6.6	6.5
0.17–0.24	8.6	8.6	8.6	8.6	8.6
0.24–0.30	12.0	12.0	12.0	12.0	11.0
0.3–0.4	15.0	16.0	16.0	15.0	15.0
0.40–0.55	20.0	20.0	20.0	20.0	20.0
0.55–0.75	26.0	26.0	26.0	26.0	25.0
0.75–1.00	32.0	32.0	32.0	32.0	32.0

of $W_{\gamma p}$. The STARLIGHT prediction is systematically higher than the data in the high- $|t|$ region. This trend becomes more significant as $W_{\gamma p}$ increases.

Figure 6 shows the differential cross section $d\sigma/d|t|$ in the rapidity interval $-1.2 < y(\pi^+\pi^-) < 0$ compared with the H1 and ZEUS results [17, 18] in a similar $W_{\gamma p}$ range.

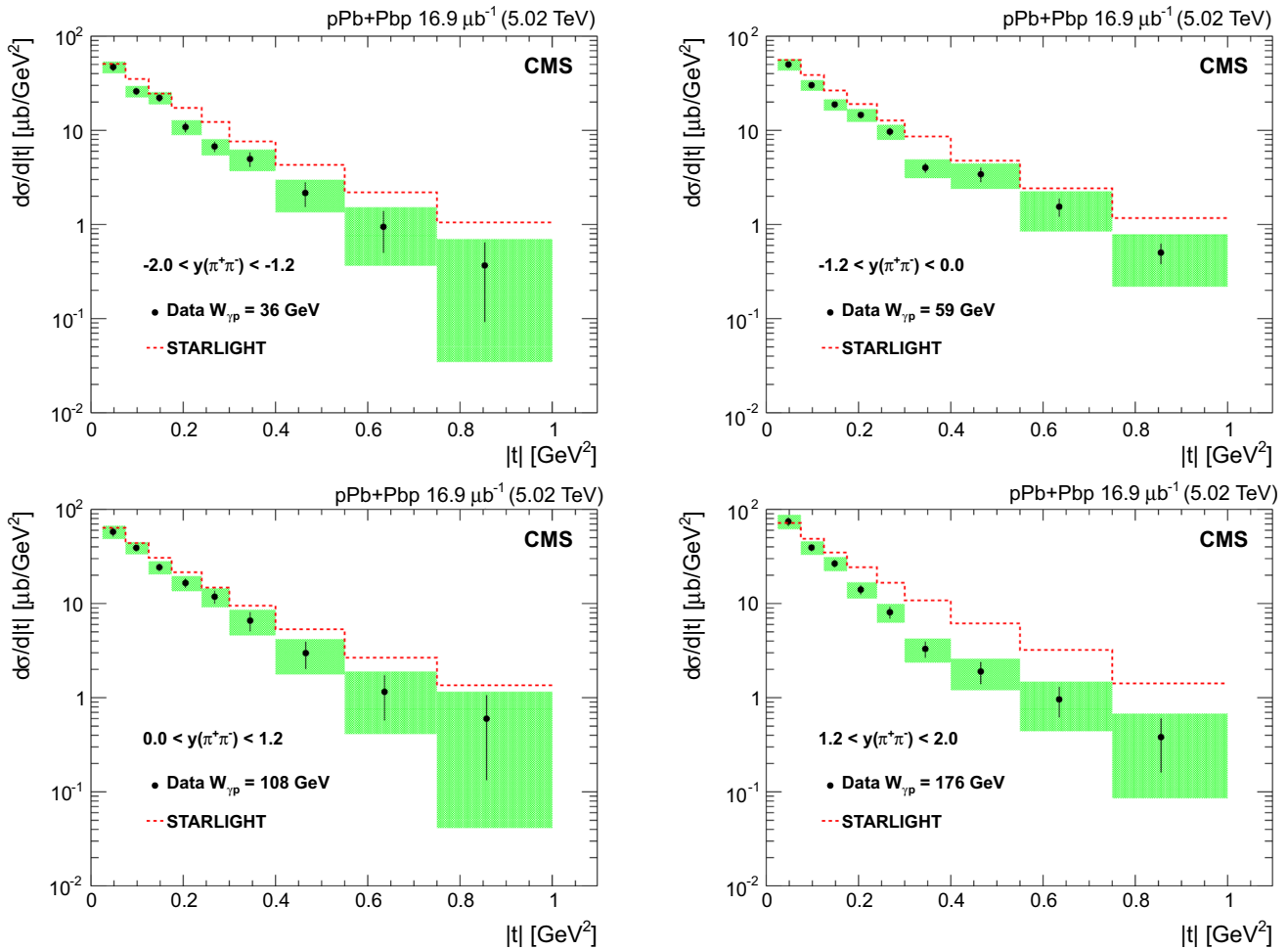


Fig. 5 Differential cross section $d\sigma/d|t|$ (full circles) in four different rapidity bins. The error bars show the statistical uncertainty, whereas the shaded areas represent the statistical and systematic uncertainties

The differential cross section as a function of $|t|$ is fitted with the form Ae^{-bt+ct^2} in the region $0.025 < |t| < 0.5 \text{ GeV}^2$. For the integrated rapidity bin the fit gives $b = 9.2 \pm 0.7$ (stat) GeV^{-2} and $c = 4.6 \pm 1.6$ (stat) GeV^{-4} . The resulting values of the slope b are shown in Fig. 7 as a function of W_{yp} , together with those measured by H1 and ZEUS [17, 18]. The values of the parameter c are found to be constant within the fit uncertainties. The Regge formula [44] $b = b_0 + 2\alpha' \ln(W_{yp}/W_0)^2$, which parametrizes the dependence of b on the collision energy, is fitted to the data using $W_0 = 92.6 \text{ GeV}$, the average centre-of-mass energy of the present data. The fit to the CMS data alone gives a pomeron slope of $\alpha' = 0.28 \pm 0.11$ (stat) ± 0.12 (syst) GeV^{-2} , consistent with the ZEUS [17] value and the Regge expectation of 0.25 GeV^{-2} .

The resulting photon–proton cross section, obtained for W_{yp} between 29 and 213 GeV ($\langle W_{yp} \rangle = 92.6 \text{ GeV}$) is extrapolated

added in quadrature. The dashed lines show the unweighted STARLIGHT predictions

to the range $0 < |t| < 0.5 \text{ GeV}^2$ using the exponential fits just discussed and the STARLIGHT predictions in order to allow direct comparison with previous experiments. The resulting value is $\sigma = 11.0 \pm 1.4$ (stat) ± 1.0 (syst) μb . The photon–proton cross section values, $\sigma(\gamma p \rightarrow \rho(770)^0 p)$, for all rapidity bins are presented in Table 3 and Fig. 8. Figure 8 also shows a compilation of fixed-target [45–48] and HERA results [17, 18]. The results of two fits are shown in Fig. 8. The dashed line indicates the result of a fit to all the plotted data with the formula $\sigma = \alpha_1 W_{yp}^{\delta_1} + \alpha_2 W_{yp}^{\delta_2}$ (see e.g. [19, 20]). The fit describes the data well and yields the values $\delta_1 = -0.81 \pm 0.04$ (stat) ± 0.09 (syst), $\delta_2 = 0.36 \pm 0.07$ (stat) ± 0.05 (syst). The CMS and HERA data are also fitted with the function $\sigma = \alpha W_{yp}^{\delta}$ as shown in Fig. 8. The fit yields $\delta = 0.24 \pm 0.13$ (stat) ± 0.04 (syst). Only statistical and uncorrelated systematic uncertainties are considered in these fits.

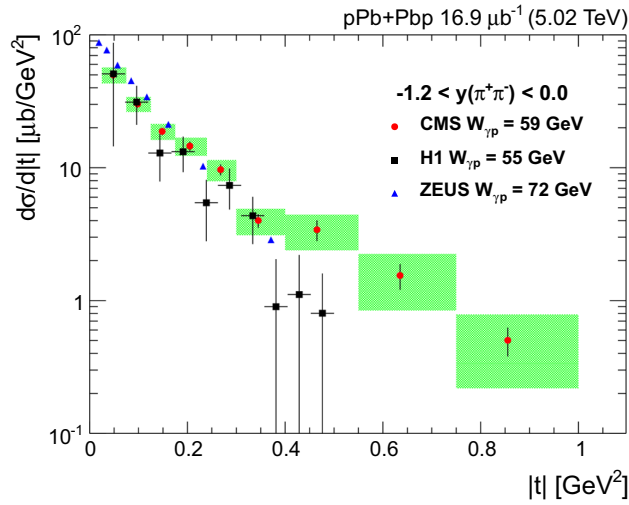


Fig. 6 Differential cross section $d\sigma/d|t|$ (full circles) for exclusive $\rho(770)^0$ photoproduction in the rapidity interval $-1.2 < y_{\pi^+\pi^-} < 0$. The square symbols indicate the H1 results, and the triangles the ZEUS results. The error bars show the statistical uncertainty, while the shaded areas represent the statistical and systematic uncertainties added in quadrature. For the H1 data [18], the error bars represent the statistical and systematic uncertainties added in quadrature, and for the ZEUS data [17] the reported uncertainties are negligible

9 Summary

The CMS Collaboration has made the first measurement of exclusive $\rho(770)^0$ photoproduction off protons in ultraperipheral pPb collisions at $\sqrt{s_{NN}} = 5.02$ TeV. The cross section for this process is measured in the photon–proton centre-

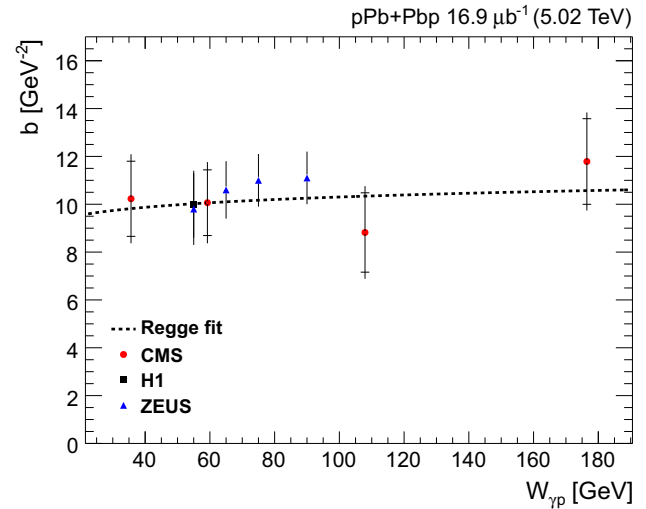


Fig. 7 The slope parameter b extracted from the exponential fits of the differential cross sections $d\sigma/d|t|$ shown as a function of $W_{\gamma p}$. The inner error bars show the statistical uncertainty, while the outer error bars indicate the statistical and systematic uncertainties added in quadrature. The dashed line shows the result of the Regge fit discussed in the text

of-mass energy interval $29 < W_{\gamma p} < 213$ GeV. The results are consistent with those of the H1 and ZEUS Collaborations at HERA, indicating that ion–proton collisions can be used in the same way as electron–proton ones, with ions acting as a source of quasi-real photons. The combination of the present data and the earlier, lower energy results agrees with theory-inspired fits. The differential cross section $d\sigma/d|t|$ for $\rho(770)^0$ photoproduction is measured as a function of $W_{\gamma p}$.

Table 3 Differential cross section for exclusive $\rho(770)^0$ photoproduction, $\sigma(\gamma p \rightarrow \rho(770)^0 p)$, with statistical and systematic uncertainties, for $|t| < 0.5$ GeV². The differential cross section $d\sigma/d|t|$ is also shown, along with the rapidity range, the average value of $W_{\gamma p}$, $\langle W_{\gamma p} \rangle$, and $k \frac{dn}{dk}$

y range	(−2.0, 2.0)	(−2.0, −1.2)	(−1.2, 0.0)	(0.0, 1.2)	(1.2, 2.0)
$W_{\gamma p}$ range [GeV]	(29, 213)	(29, 43)	(43, 78)	(78, 143)	(143, 213)
$\langle W_{\gamma p} \rangle$ [GeV]	92.6	35.6	59.2	108.0	176.0
$k \frac{dn}{dk}$	136.0	186.0	155.0	117.0	86.2
$d\sigma/dy$ [μb]	11.0	9.1	9.9	12.4	12.9
Stat. unc. [μb]	1.4	1.5	1.6	2.4	2.6
Syst. unc. [μb]	1.0	0.8	0.9	1.1	1.3
$ t $ [GeV ²]	$d\sigma/d t $ [μb/GeV ²]	$d\sigma/d t $ [μb/GeV ²]	$d\sigma/d t $ [μb/GeV ²]	$d\sigma/d t $ [μb/GeV ²]	$d\sigma/d t $ [μb/GeV ²]
0.025–0.075	$56.0 \pm 2.2 \pm 6.4$	$47.0 \pm 4.5 \pm 4.9$	$50.0 \pm 4.1 \pm 5.5$	$57.7 \pm 6.1 \pm 6.9$	$74.5 \pm 7.9 \pm 10.2$
0.075–0.125	$33.6 \pm 1.0 \pm 3.9$	$26.0 \pm 2.3 \pm 2.8$	$30.2 \pm 1.9 \pm 3.4$	$39.1 \pm 3.2 \pm 4.7$	$39.3 \pm 3.4 \pm 5.5$
0.125–0.175	$24.4 \pm 0.8 \pm 3.0$	$22.1 \pm 2.1 \pm 2.6$	$18.8 \pm 1.2 \pm 2.3$	$24.3 \pm 2.2 \pm 3.1$	$26.6 \pm 2.3 \pm 3.9$
0.175–0.240	$15.5 \pm 0.7 \pm 2.1$	$10.9 \pm 1.3 \pm 1.4$	$14.6 \pm 1.2 \pm 2.0$	$16.5 \pm 1.9 \pm 2.4$	$14.1 \pm 1.7 \pm 2.2$
0.24–0.30	$10.2 \pm 0.6 \pm 1.6$	$6.7 \pm 0.8 \pm 1.0$	$9.7 \pm 0.9 \pm 1.5$	$11.8 \pm 1.9 \pm 1.9$	$8.1 \pm 1.1 \pm 1.4$
0.3–0.4	$5.2 \pm 0.4 \pm 1.4$	$5.0 \pm 0.9 \pm 1.4$	$4.0 \pm 0.5 \pm 1.4$	$6.6 \pm 1.5 \pm 1.4$	$3.3 \pm 0.6 \pm 1.4$
0.40–0.55	$3.5 \pm 0.4 \pm 1.4$	$2.2 \pm 0.6 \pm 1.4$	$3.4 \pm 0.6 \pm 1.4$	$3.0 \pm 1.0 \pm 1.4$	$1.9 \pm 0.5 \pm 1.4$
0.55–0.75	$1.4 \pm 0.3 \pm 1.4$	$0.94 \pm 0.44 \pm 1.4$	$1.5 \pm 0.3 \pm 1.4$	$1.2 \pm 0.6 \pm 1.4$	$1.0 \pm 0.3 \pm 1.4$
0.75–1.00	$0.52 \pm 0.14 \pm 1.4$	$0.37 \pm 0.28 \pm 1.4$	$0.50 \pm 0.12 \pm 1.4$	$0.60 \pm 0.47 \pm 1.4$	$0.38 \pm 0.22 \pm 1.4$

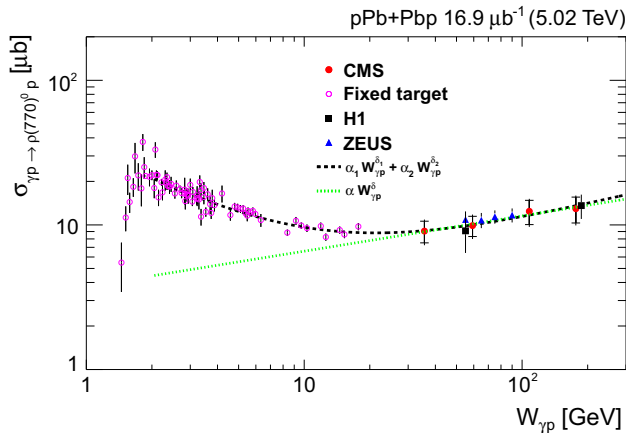


Fig. 8 Exclusive $\rho(770)^0$ photoproduction cross section as a function of W_{yp} . The inner bars show the statistical uncertainty, while the outer bars represent the statistical and systematic uncertainties added in quadrature. Fixed-target [45–48] and HERA [17, 18] data are also shown. The dashed lines indicate the results of the fits described in the text

The STARLIGHT prediction is systematically higher than the data in the high- $|t|$ region. This trend becomes more significant as W_{yp} increases.

Acknowledgements We congratulate our colleagues in the CERN accelerator departments for the excellent performance of the LHC and thank the technical and administrative staffs at CERN and at other CMS institutes for their contributions to the success of the CMS effort. In addition, we gratefully acknowledge the computing centres and personnel of the Worldwide LHC Computing Grid for delivering so effectively the computing infrastructure essential to our analyses. Finally, we acknowledge the enduring support for the construction and operation of the LHC and the CMS detector provided by the following funding agencies: BMWFW and FWF (Austria); FNRS and FWO (Belgium); CNPq, CAPES, FAPERJ, and FAPESP (Brazil); MES (Bulgaria); CERN; CAS, MoST, and NSFC (China); COLCIENCIAS (Colombia); MSES and CSF (Croatia); RPF (Cyprus); SENESCYT (Ecuador); MoER, ERC IUT and ERDF (Estonia); Academy of Finland, MEC, and HIP (Finland); CEA and CNRS/IN2P3 (France); BMBF, DFG, and HGF (Germany); GSRT (Greece); OTKA and NIH (Hungary); DAE and DST (India); IPM (Iran); SFI (Ireland); INFN (Italy); MSIP and NRF (Republic of Korea); LAS (Lithuania); MOE and UM (Malaysia); BUAP, CINVESTAV, CONACYT, LNS, SEP, and UASLP-FAI (Mexico); MBIE (New Zealand); PAEC (Pakistan); MSHE and NSC (Poland); FCT (Portugal); JINR (Dubna); MON, RosAtom, RAS and RFBR (Russia); MESTD (Serbia); SEIDI and CPAN (Spain); Swiss Funding Agencies (Switzerland); MST (Taipei); ThEPCenter, IPST, STAR and NSTDA (Thailand); TUBITAK and TAEC (Turkey); NASU and SFFR (Ukraine); STFC (UK); DOE and NSF (USA). Individuals have received support from the Marie-Curie programme and the European Research Council and Horizon 2020 Grant, contract No. 675440 (European Union); the Leventis Foundation; the A.P. Sloan Foundation; the Alexander von Humboldt Foundation; the Belgian Federal Science Policy Office; the Fonds pour la Formation à la Recherche dans l’Industrie et dans l’Agriculture (FRIA-Belgium); the Agentschap voor Innovatie door Wetenschap en Technologie (IWT-Belgium); the F.R.S.-FNRS and FWO (Belgium) under the “Excellence of Science – EOS” – be.h project n. 30820817; the Ministry of Education, Youth and Sports (MEYS) of the Czech Republic; the Lendület (“Momentum”) Programme and the János Bolyai Research Scholarship of the

Hungarian Academy of Sciences, the New National Excellence Program ÚNKP, the NKFI research Grants 123842, 123959, 124845, 124850, and 125105 (Hungary); the Council of Science and Industrial Research, India; the HOMING PLUS programme of the Foundation for Polish Science, cofinanced from European Union, Regional Development Fund, the Mobility Plus programme of the Ministry of Science and Higher Education, the National Science Center (Poland), contracts Harmonia 2014/14/M/ST2/00428, Opus 2014/13/B/ST2/02543, 2014/15/B/ST2/03998, and 2015/19/B/ST2/02861, Sonata-bis 2012/07/E/ST2/01406; the National Priorities Research Program by Qatar National Research Fund; the Programa Estatal de Fomento de la Investigación Científica y Técnica de Excelencia María de Maeztu, Grant MDM-2015-0509 and the Programa Severo Ochoa del Principado de Asturias; the Thalís and Aristeia programmes cofinanced by EU-ESF and the Greek NSRF; the Rachadapisek Sompot Fund for Postdoctoral Fellowship, Chulalongkorn University and the Chulalongkorn Academic into Its 2nd Century Project Advancement Project (Thailand); the Welch Foundation, contract C-1845; and the Weston Havens Foundation (USA).

Data Availability Statement This manuscript has no associated data or the data will not be deposited. [Authors’ comment: Release and preservation of data used by the CMS Collaboration as the basis for publications is guided by the CMS policy as written in its document “CMS data preservation, re-use and open access policy” (<https://cmsdocdb.cern.ch/cgi-bin/PublicDocDB/RetrieveFile?docid=6032&filename=CMSDataPolicyV1.2.pdf&version=2>).]

Open Access This article is distributed under the terms of the Creative Commons Attribution 4.0 International License (<http://creativecommons.org/licenses/by/4.0/>), which permits unrestricted use, distribution, and reproduction in any medium, provided you give appropriate credit to the original author(s) and the source, provide a link to the Creative Commons license, and indicate if changes were made.

Funded by SCOAP³.

References

1. A.J. Baltz, The physics of ultraperipheral collisions at the LHC. Phys. Rept. **458**, 1 (2008). <https://doi.org/10.1016/j.physrep.2007.12.001>. arXiv:0706.3356
2. J.G. Contreras, J.D. Tapia Takaki, Ultra-peripheral heavy-ion collisions at the LHC. Int. J. Mod. Phys. A **30**, 1542012 (2015). <https://doi.org/10.1142/S0217751X15420129>
3. L. Frankfurt, M. Strikman, M. Zhalov, Elastic and large t rapidity gap vector meson production in ultraperipheral proton–ion collisions. Phys. Lett. B **640**, 162 (2006). <https://doi.org/10.1016/j.physletb.2006.07.059>. arXiv:hep-ph/0605160
4. V. Guzey, M. Zhalov, Rapidity and momentum transfer distributions of coherent J/ψ photoproduction in ultraperipheral pPb collisions at the LHC. JHEP **02**, 046 (2014). [https://doi.org/10.1007/JHEP02\(2014\)046](https://doi.org/10.1007/JHEP02(2014)046). arXiv:1307.6689
5. N. Armesto, A.H. Rezaeian, Exclusive vector meson production at high energies and gluon saturation. Phys. Rev. D **90**, 054003 (2014). <https://doi.org/10.1103/PhysRevD.90.054003>. arXiv:1402.4831
6. T. Toll, T. Ullrich, Exclusive diffractive processes in electron–ion collisions. Phys. Rev. C **87**, 024913 (2013). <https://doi.org/10.1103/PhysRevC.87.024913>. arXiv:1211.3048
7. S.P. Jones, A.D. Martin, M.G. Ryskin, T. Teubner, Probes of the small x gluon via exclusive J/ψ and Υ production at HERA and the LHC. JHEP **11**, 085 (2013). [https://doi.org/10.1007/JHEP11\(2013\)085](https://doi.org/10.1007/JHEP11(2013)085). arXiv:1307.7099

8. V.P. Goncalves, F.S. Navarra, D. Spiering, Exclusive $\rho(770)$ and J/ψ photoproduction in ultraperipheral pA collisions: predictions of the gluon saturation models for the momentum transfer distributions. *Phys. Lett. B* **791**, 299 (2019). <https://doi.org/10.1016/j.physletb.2019.03.007>. arXiv:1811.09124
9. J. Cepila, J.G. Contreras, M. Krelina, J.D.Tapia Takaki, Mass dependence of vector meson photoproduction off protons and nuclei within the energy-dependent hot-spot model. *Nucl. Phys. B* **934**, 330 (2018). <https://doi.org/10.1016/j.nuclphysb.2018.07.010>. arXiv:1804.05508
10. J. Cepila, J.G. Contreras, J.D.Tapia Takaki, Energy dependence of dissociative J/ψ photoproduction as a signature of gluon saturation at the LHC. *Phys. Lett. B* **766**, 186 (2017). <https://doi.org/10.1016/j.physletb.2016.12.063>. arXiv:1608.07559
11. ALICE Collaboration, Exclusive J/ψ photoproduction off protons in ultraperipheral p–Pb collisions at $\sqrt{s_{NN}} = 5.02$ TeV. *Phys. Rev. Lett.* **113**, 232504 (2014). <https://doi.org/10.1103/PhysRevLett.113.232504>. arXiv:1406.7819
12. ALICE Collaboration, Coherent J/ψ photoproduction in ultraperipheral Pb–Pb collisions at $\sqrt{s_{NN}} = 2.76$ TeV. *Phys. Lett. B* **718**, 1273 (2013). <https://doi.org/10.1016/j.physletb.2012.11.059>. arXiv:1209.3715
13. LHCb Collaboration, Updated measurements of exclusive J/ψ and $\psi(2s)$ production cross-sections in pp collisions at $\sqrt{s} = 7$ TeV. *J. Phys. G* **41**, 055002 (2014). <https://doi.org/10.1088/0954-3899/41/5/055002>. arXiv:1401.3288
14. LHCb Collaboration, Measurement of the exclusive Y production cross-section in pp collisions at $\sqrt{s} = 7$ TeV and 8 TeV. *JHEP* **09**, 084 (2015). [https://doi.org/10.1007/JHEP09\(2015\)084](https://doi.org/10.1007/JHEP09(2015)084). arXiv:1505.08139
15. T.H. Bauer, R.D. Spital, D.R. Yennie, F.M. Pipkin, The hadronic properties of the photon in high-energy interactions. *Rev. Mod. Phys.* **50**, 261 (1978). <https://doi.org/10.1103/RevModPhys.50.261>. [Erratum: <https://doi.org/10.1103/RevModPhys.51.407>]
16. J.A. Crittenden, Exclusive production of neutral vector mesons at the electron–proton collider HERA. PhD thesis, Physikalisches Institut der Universitaet Bonn (1997). arXiv:hep-ex/9704009. DESY-97-068, BONN-IR-97-01
17. ZEUS Collaboration, Elastic and proton dissociative ρ^0 photoproduction at HERA. *Eur. Phys. J. C* **2**, 247 (1998). <https://doi.org/10.1007/s100529800834>. arXiv:hep-ex/9712020
18. H1 Collaboration, Elastic photoproduction of ρ^0 mesons at HERA. *Nucl. Phys. B* **463**, 3 (1996). [https://doi.org/10.1016/0550-3213\(96\)00045-4](https://doi.org/10.1016/0550-3213(96)00045-4). arXiv:hep-ex/9601004
19. P. Newman, M. Wing, The hadronic final state at HERA. *Rev. Mod. Phys.* **86**, 1037 (2014). <https://doi.org/10.1103/RevModPhys.86.1037>. arXiv:1308.3368
20. L. Favart, M. Guidal, T. Horn, P. Kroll, Deeply virtual meson production on the nucleon. *Eur. Phys. J. A* **52**, 158 (2016). <https://doi.org/10.1140/epja/i2016-16158-2>. arXiv:1511.04535
21. STAR Collaboration, Coherent ρ^0 production in ultraperipheral heavy ion collisions. *Phys. Rev. Lett.* **89**, 272302 (2002). <https://doi.org/10.1103/PhysRevLett.89.272302>. arXiv:nucl-ex/0206004
22. STAR Collaboration, ρ^0 photoproduction in ultraperipheral relativistic heavy ion collisions at $\sqrt{s_{NN}} = 200$ GeV. *Phys. Rev. C* **77**, 034910 (2008). <https://doi.org/10.1103/PhysRevC.77.034910>. arXiv:0712.3320
23. STAR Collaboration, Coherent diffractive photoproduction of ρ^0 mesons on gold nuclei at 200 GeV/nucleon-pair at the relativistic heavy ion collider. *Phys. Rev. C* **96**, 054904 (2017). <https://doi.org/10.1103/PhysRevC.96.054904>. arXiv:1702.07705
24. ALICE Collaboration, Coherent ρ^0 photoproduction in ultraperipheral Pb–Pb collisions at $\sqrt{s_{NN}} = 2.76$ TeV. *JHEP* **09**, 095 (2015). [https://doi.org/10.1007/JHEP09\(2015\)095](https://doi.org/10.1007/JHEP09(2015)095). arXiv:1503.09177
25. L. Frankfurt, V. Guzey, M. Strikman, M. Zhalov, Nuclear shadowing in photoproduction of $\rho(770)^0$ mesons in ultraperipheral nucleus collisions at RHIC and the LHC. *Phys. Lett. B* **752**, 51 (2016). <https://doi.org/10.1016/j.physletb.2015.11.012>. arXiv:1506.07150
26. CMS Collaboration, Description and performance of track and primary-vertex reconstruction with the CMS tracker. *JINST* **9**, P10009 (2014). <https://doi.org/10.1088/1748-0221/9/10/P10009>. arXiv:1405.6569
27. CMS Collaboration, The CMS experiment at the CERN LHC. *JINST* **3**, S08004 (2008). <https://doi.org/10.1088/1748-0221/3/08/S08004>
28. S.R. Klein et al., STARLIGHT: a Monte Carlo simulation program for ultra-peripheral collisions of relativistic ions. *Comput. Phys. Commun.* **212**, 258 (2017). <https://doi.org/10.1016/j.cpc.2016.10.016>. arXiv:1607.03838
29. GEANT4 Collaboration, Geant4—a simulation toolkit. *Nucl. Instrum. Methods A* **506**, 250 (2003). [https://doi.org/10.1016/S0168-9002\(03\)01368-8](https://doi.org/10.1016/S0168-9002(03)01368-8)
30. CMS Collaboration, The CMS trigger system. *JINST* **12**, P01020 (2017). <https://doi.org/10.1088/1748-0221/12/01/P01020>. arXiv:1609.02366
31. CMS Collaboration, CMS tracking performance results from early LHC operation. *Eur. Phys. J. C* **70**, 1165 (2010). <https://doi.org/10.1140/epjc/s10052-010-1491-3>. arXiv:1007.1988
32. H1 Collaboration, Diffractive electroproduction of ρ and ϕ mesons at HERA. *JHEP* **05**, 032 (2010). [https://doi.org/10.1007/JHEP05\(2010\)032](https://doi.org/10.1007/JHEP05(2010)032). arXiv:0910.5831
33. Particle Data Group, M. Tanabashi et al., Review of particle physics. *Phys. Rev. D* **98** 030001 (2018). <https://doi.org/10.1103/PhysRevD.98.030001>
34. STAR Collaboration, Observation of $\pi^+\pi^-\pi^+\pi^-$ photoproduction in ultraperipheral heavy-ion Collisions at STAR. *Phys. Rev. C* **81**, 044901 (2010). <https://doi.org/10.1103/PhysRevC.81.044901>. arXiv:0912.0604
35. A.J. Schramm, D.H. Reeves, Production of η mesons in double Pomeron exchange. *Phys. Rev. D* **55**, 7312 (1997). <https://doi.org/10.1103/PhysRevD.55.7312>. arXiv:hep-ph/9611330
36. G. D’Agostini, A multidimensional unfolding method based on Bayes theorem. *Nucl. Instrum. Methods A* **362**, 487 (1995). [https://doi.org/10.1016/0168-9002\(95\)00274-X](https://doi.org/10.1016/0168-9002(95)00274-X)
37. T. Adye, Unfolding algorithms and tests using RooUnfold. In Proceedings, PHYSTAT 2011 Workshop on Statistical Issues Related to Discovery Claims in Search Experiments and Unfolding, CERN, Geneva, Switzerland 17–20 January 2011, p. 313, CERN. CERN, Geneva, (2011). arXiv:1105.1160. <https://doi.org/10.5170/CERN-2011-006.313>
38. G. McClellan et al., Photoproduction of neutral ρ^0 mesons. *Phys. Rev. D* **4**, 2683 (1971). <https://doi.org/10.1103/PhysRevD.4.2683>
39. P. Söding, On the apparent shift of the ρ meson mass in photoproduction. *Phys. Lett.* **19**, 702 (1966). [https://doi.org/10.1016/0031-9163\(66\)90451-3](https://doi.org/10.1016/0031-9163(66)90451-3)
40. H. Alvensleben et al., Precise determination of rho-omega interference parameters from photoproduction of vector mesons off nucleon and nuclei. *Phys. Rev. Lett.* **27**, 888 (1971). <https://doi.org/10.1103/PhysRevLett.27.888>
41. CMS Collaboration, Luminosity calibration for the 2013 proton–lead and proton–proton data taking. CMS Physics Analysis Summary CMS-PAS-LUM-13-002 (2013)
42. CMS Collaboration, Measurement of the inclusive energy spectrum in the very forward direction in proton–proton collisions at $\sqrt{s} = 13$ TeV. *JHEP* **08**, 046 (2017). [https://doi.org/10.1007/JHEP08\(2017\)046](https://doi.org/10.1007/JHEP08(2017)046). arXiv:1701.08695

43. M.H. Ross, L. Stodolsky, Photon dissociation model for vector meson photoproduction. *Phys. Rev.* **149**, 1172 (1966). <https://doi.org/10.1103/PhysRev.149.1172>
44. K.A. Goulianos, Diffractive interactions of hadrons at high energies. *Phys. Rept.* **101**, 169 (1983). [https://doi.org/10.1016/0370-1573\(83\)90010-8](https://doi.org/10.1016/0370-1573(83)90010-8)
45. E665 Collaboration, Diffractive production of $\rho^0(770)$ mesons in muon–proton interactions at 470-GeV. *Z. Phys. C* **74**, 237 (1997). <https://doi.org/10.1007/s002880050386>
46. D.G. Cassel et al., Exclusive ρ^0 , ω and ϕ electroproduction. *Phys. Rev. D* **24**, 2787 (1981). <https://doi.org/10.1103/PhysRevD.24.2787>
47. CLAS Collaboration, Exclusive ρ^0 meson electroproduction from hydrogen at CLAS. *Phys. Lett. B* **605**, 256 (2005). <https://doi.org/10.1016/j.physletb.2004.11.019>. [arXiv:hep-ex/0408005](https://arxiv.org/abs/hep-ex/0408005)
48. CLAS Collaboration, Exclusive ρ^0 electroproduction on the proton at CLAS. *Eur. Phys. J. A* **39**, 5 (2009). <https://doi.org/10.1140/epja/i2008-10683-5>. [arXiv:0807.3834](https://arxiv.org/abs/0807.3834)

CMS Collaboration

Yerevan Physics Institute, Yerevan, Armenia

A. M. Sirunyan, A. Tumasyan

Institut für Hochenergiephysik, Wien, Austria

W. Adam, F. Ambrogio, E. Asilar, T. Bergauer, J. Brandstetter, M. Dragicevic, J. Erö, A. Escalante Del Valle, M. Flechl, R. Frühwirth¹, V. M. Ghete, J. Hrubec, M. Jeitler¹, N. Krammer, I. Krätschmer, D. Liko, T. Madlener, I. Mikulec, N. Rad, H. Rohringer, J. Schieck¹, R. Schöfbeck, M. Spanring, D. Spitzbart, A. Taurok, W. Waltenberger, J. Wittmann, C.-E. Wulz¹, M. Zarucki

Institute for Nuclear Problems, Minsk, Belarus

V. Chekhovsky, V. Mossolov, J. Suarez Gonzalez

Universiteit Antwerpen, Antwerp, Belgium

E. A. De Wolf, D. Di Croce, X. Janssen, J. Lauwers, M. Pieters, M. Van De Klundert, H. Van Haeveermaet, P. Van Mechelen, N. Van Remortel

Vrije Universiteit Brussel, Brussels, Belgium

S. Abu Zeid, F. Blekman, J. D'Hondt, I. De Bruyn, J. De Clercq, K. Deroover, G. Flouris, D. Lontkovskyi, S. Lowette, I. Marchesini, S. Moortgat, L. Moreels, Q. Python, K. Skovpen, S. Tavernier, W. Van Doninck, P. Van Mulders, I. Van Parijs

Université Libre de Bruxelles, Brussels, Belgium

D. Beghin, B. Bilin, H. Brun, B. Clerbaux, G. De Lentdecker, H. Delannoy, B. Dorney, G. Fasanella, L. Favart, R. Goldouzian, A. Grebenyuk, A. K. Kalsi, T. Lenzi, J. Luetic, L. Moureaux, N. Postiau, E. Starling, L. Thomas, C. Vander Velde, P. Vanlaer, D. Vannerom, Q. Wang

Ghent University, Ghent, Belgium

T. Cornelis, D. Dobur, A. Fagot, M. Gul, I. Khvastunov², D. Poyraz, C. Roskas, D. Trocino, M. Tytgat, W. Verbeke, B. Vermassen, M. Vit, N. Zaganidis

Université Catholique de Louvain, Louvain-la-Neuve, Belgium

H. Bakhshiansohi, O. Bondu, S. Brochet, G. Bruno, C. Caputo, P. David, C. Delaere, M. Delcourt, B. Francois, A. Giammanco, G. Krintiras, V. Lemaitre, A. Magitteri, A. Mertens, M. Musich, K. Piotrkowski, A. Saggio, M. Vidal Marono, S. Wertz, J. Zobec

Centro Brasileiro de Pesquisas Fisicas, Rio de Janeiro, Brazil

F. L. Alves, G. A. Alves, L. Brito, G. Correia Silva, C. Hensel, A. Moraes, M. E. Pol, P. Rebello Teles

Universidade do Estado do Rio de Janeiro, Rio de Janeiro, Brazil

E. Belchior Batista Das Chagas, W. Carvalho, J. Chinellato³, E. Coelho, E. M. Da Costa, G. G. Da Silveira⁴, D. De Jesus Damiao, C. De Oliveira Martins, S. Fonseca De Souza, H. Malbouisson, D. Matos Figueiredo, M. Melo De Almeida, C. Mora Herrera, L. Mundim, H. Nogima, W. L. Prado Da Silva, L. J. Sanchez Rosas, A. Santoro, A. Sznajder, M. Thiel, E. J. Tonelli Manganote³, F. Torres Da Silva De Araujo, A. Vilela Pereira

Universidade Estadual Paulista^a, Universidade Federal do ABC^b, São Paulo, Brazil

S. Ahuja^a, C. A. Bernardes^a, L. Calligaris^a, T. R. Fernandez Perez Tomei^a, E. M. Gregores^b, P. G. Mercadante^b, S. F. Novaes^a, Sandra S. Padula^a, D. Romero Abad^b

Institute for Nuclear Research and Nuclear Energy, Bulgarian Academy of Sciences, Sofia, Bulgaria

A. Aleksandrov, R. Hadjiiska, P. Iaydjiev, A. Marinov, M. Misheva, M. Rodozov, M. Shopova, G. Sultanov

University of Sofia, Sofia, Bulgaria

A. Dimitrov, L. Litov, B. Pavlov, P. Petkov

Beihang University, Beijing, China

W. Fang⁵, X. Gao⁵, L. Yuan

Institute of High Energy Physics, Beijing, China

M. Ahmad, J. G. Bian, G. M. Chen, H. S. Chen, M. Chen, Y. Chen, C. H. Jiang, D. Leggat, H. Liao, Z. Liu, F. Romeo, S. M. Shaheen⁶, A. Spiezia, J. Tao, C. Wang, Z. Wang, E. Yazgan, H. Zhang, J. Zhao

State Key Laboratory of Nuclear Physics and Technology, Peking University, Beijing, China

Y. Ban, G. Chen, A. Levin, J. Li, L. Li, Q. Li, Y. Mao, S. J. Qian, D. Wang, Z. Xu

Tsinghua University, Beijing, China

Y. Wang

Universidad de Los Andes, Bogotá, Colombia

C. Avila, A. Cabrera, C. A. Carrillo Montoya, L. F. Chaparro Sierra, C. Florez, C. F. González Hernández, M. A. Segura Delgado

University of Split, Faculty of Electrical Engineering, Mechanical Engineering and Naval Architecture, Split, Croatia

B. Courbon, N. Godinovic, D. Lelas, I. Puljak, T. Sculac

University of Split, Faculty of Science, Split, Croatia

Z. Antunovic, M. Kovac

Institute Rudjer Boskovic, Zagreb, Croatia

V. Brigljevic, D. Ferencek, K. Kadija, B. Mesic, A. Starodumov⁷, T. Susa

University of Cyprus, Nicosia, Cyprus

M. W. Ather, A. Attikis, M. Kolosova, G. Mavromanolakis, J. Mousa, C. Nicolaou, F. Ptochos, P. A. Razis, H. Rykaczewski

Charles University, Prague, Czech Republic

M. Finger⁸, M. Finger Jr.⁸

Escuela Politécnica Nacional, Quito, Ecuador

E. Ayala

Universidad San Francisco de Quito, Quito, Ecuador

E. Carrera Jarrin

Academy of Scientific Research and Technology of the Arab Republic of Egypt, Egyptian Network of High Energy Physics, Cairo, Egypt

A. Ellithi Kamel⁹, M. A. Mahmoud^{10,11}, E. Salama^{11,12}

National Institute of Chemical Physics and Biophysics, Tallinn, Estonia

S. Bhowmik, A. Carvalho Antunes De Oliveira, R. K. Dewanjee, K. Ehataht, M. Kadastik, M. Raidal, C. Veelken

Department of Physics, University of Helsinki, Helsinki, Finland

P. Eerola, H. Kirschenmann, J. Pekkanen, M. Voutilainen

Helsinki Institute of Physics, Helsinki, Finland

J. Havukainen, J. K. Heikkilä, T. Järvinen, V. Karimäki, R. Kinnunen, T. Lampén, K. Lassila-Perini, S. Laurila, S. Lehti, T. Lindén, P. Luukka, T. Mäenpää, H. Siikonen, E. Tuominen, J. Tuominiemi

Lappeenranta University of Technology, Lappeenranta, Finland

T. Tuuva

IRFU, CEA, Université Paris-Saclay, Gif-sur-Yvette, France

M. Besancon, F. Couderc, M. Dejardin, D. Denegri, J. L. Faure, F. Ferri, S. Ganjour, A. Givernaud, P. Gras,

G. Hamel de Monchenault, P. Jarry, C. Leloup, E. Locci, J. Malcles, G. Negro, J. Rander, A. Rosowsky, M. Ö. Sahin, M. Titov

Laboratoire Leprince-Ringuet, Ecole polytechnique, CNRS/IN2P3, Université Paris-Saclay, Palaiseau, France

A. Abdulsalam¹³, C. Amendola, I. Antropov, F. Beaudette, P. Busson, C. Charlot, R. Granier de Cassagnac, I. Kucher, S. Lisniak, A. Lobanov, J. Martin Blanco, M. Nguyen, C. Ochando, G. Ortona, P. Paganini, P. Pigard, R. Salerno, J. B. Sauvan, Y. Sirois, A. G. Stahl Leiton, A. Zabi, A. Zghiche

Université de Strasbourg, CNRS, IPHC UMR 7178, Strasbourg, France

J.-L. Agram¹⁴, J. Andrea, D. Bloch, J.-M. Brom, E. C. Chabert, V. Cherepanov, C. Collard, E. Conte¹⁴, J.-C. Fontaine¹⁴, D. Gelé, U. Goerlach, M. Jansová, A.-C. Le Bihan, N. Tonon, P. Van Hove

Centre de Calcul de l'Institut National de Physique Nucleaire et de Physique des Particules, CNRS/IN2P3, Villeurbanne, France

S. Gadrat

Université de Lyon, Université Claude Bernard Lyon 1, CNRS-IN2P3, Institut de Physique Nucléaire de Lyon, Villeurbanne, France

S. Beauceron, C. Bernet, G. Boudoul, N. Chanon, R. Chierici, D. Contardo, P. Depasse, H. El Mamouni, J. Fay, L. Finco, S. Gascon, M. Gouzevitch, G. Grenier, B. Ille, F. Lagarde, I. B. Laktineh, H. Lattaud, M. Lethuillier, L. Mirabito, A. L. Pequegnot, S. Perries, A. Popov¹⁵, V. Sordini, M. Vander Donckt, S. Viret, S. Zhang

Georgian Technical University, Tbilisi, Georgia

A. Khvedelidze⁸

Tbilisi State University, Tbilisi, Georgia

I. Bagaturia¹⁶

RWTH Aachen University, I. Physikalisches Institut, Aachen, Germany

C. Autermann, L. Feld, M. K. Kiesel, K. Klein, M. Lipinski, M. Preuten, M. P. Rauch, C. Schomakers, J. Schulz, M. Teroerde, B. Wittmer, V. Zhukov¹⁵

RWTH Aachen University, III. Physikalisches Institut A, Aachen, Germany

A. Albert, D. Duchardt, M. Endres, M. Erdmann, T. Esch, R. Fischer, S. Ghosh, A. Güth, T. Hebbeker, C. Heidemann, K. Hoepfner, H. Keller, S. Knutzen, L. Mastrolorenzo, M. Merschmeyer, A. Meyer, P. Millet, S. Mukherjee, T. Pook, M. Radziej, H. Reithler, M. Rieger, F. Scheuch, A. Schmidt, D. Teyssier

RWTH Aachen University, III. Physikalisches Institut B, Aachen, Germany

G. Flügge, O. Hlushchenko, B. Kargoll, T. Kress, A. Künsken, T. Müller, A. Nehr Korn, A. Nowack, C. Pistone, O. Pooth, H. Sert, A. Stahl¹⁷

Deutsches Elektronen-Synchrotron, Hamburg, Germany

M. Aldaya Martin, T. Arndt, C. Asawatangtrakuldee, I. Babounikau, K. Beernaert, O. Behnke, U. Behrens, A. Bermúdez Martínez, D. Bertsche, A. A. Bin Anuar, K. Borras¹⁸, V. Botta, A. Campbell, P. Connor, C. Contreras-Campana, F. Costanza, V. Danilov, A. De Wit, M. M. Defranchis, C. Diez Pardos, D. Domínguez Damiani, G. Eckerlin, T. Eichhorn, A. Elwood, E. Eren, E. Gallo¹⁹, A. Geiser, J. M. Grados Luyando, A. Grohsjean, P. Gunnellini, M. Guthoff, M. Haranko, A. Harb, J. Hauk, H. Jung, M. Kasemann, J. Keaveney, C. Kleinwort, J. Knolle, D. Krücker, W. Lange, A. Lelek, T. Lenz, K. Lipka, W. Lohmann²⁰, R. Mankel, I.-A. Melzer-Pellmann, A. B. Meyer, M. Meyer, M. Missiroli, G. Mittag, J. Mnich, V. Myronenko, S. K. Pflitsch, D. Pitzl, A. Raspereza, M. Savitskyi, P. Saxena, P. Schütze, C. Schwanenberger, R. Shevchenko, A. Singh, N. Stefaniuk, H. Tholen, O. Turkot, A. Vagnerini, G. P. Van Onsem, R. Walsh, Y. Wen, K. Wichmann, C. Wissing, O. Zenaiev

University of Hamburg, Hamburg, Germany

R. Aggleton, S. Bein, L. Benato, A. Benecke, V. Blobel, M. Centis Vignali, T. Dreyer, E. Garutti, D. Gonzalez, J. Haller, A. Hinzmann, A. Karavdina, G. Kasieczka, R. Klanner, R. Kogler, N. Kovalchuk, S. Kurz, V. Kutzner, J. Lange, D. Marconi, J. Multhaupt, M. Niedziela, D. Nowatschin, A. Perieanu, A. Reimers, O. Rieger, C. Scharf, P. Schleper, S. Schumann, J. Schwandt, J. Sonneveld, H. Stadie, G. Steinbrück, F. M. Stober, M. Stöver, D. Troendle, A. Vanhoefer, B. Vormwald

Karlsruher Institut fuer Technologie, Karlsruhe, Germany

M. Akbiyik, C. Barth, M. Baselga, S. Baur, E. Butz, R. Caspart, T. Chwalek, F. Colombo, W. De Boer, A. Dierlamm, N. Faltermann, B. Freund, M. Giffels, M. A. Harrendorf, F. Hartmann¹⁷, S. M. Heindl, U. Husemann, F. Kassel¹⁷, I. Katkov¹⁵, S. Kudella, H. Mildner, S. Mitra, M. U. Mozer, Th. Müller, M. Plagge, G. Quast, K. Rabbertz, M. Schröder, I. Shvetsov, G. Sieber, H. J. Simonis, R. Ulrich, S. Wayand, M. Weber, T. Weiler, S. Williamson, C. Wöhrmann, R. Wolf

Institute of Nuclear and Particle Physics (INPP), NCSR Demokritos, Aghia Paraskevi, Greece

G. Anagnostou, G. Daskalakis, T. Geralis, A. Kyriakis, D. Loukas, G. Paspalaki, I. Topsis-Giotis

National and Kapodistrian University of Athens, Athens, Greece

G. Karathanasis, S. Kesiosoglou, P. Kontaxakis, A. Panagiotou, N. Saoulidou, E. Tziaferi, K. Vellidis

National Technical University of Athens, Athens, Greece

K. Kousouris, I. Papakrivopoulos, G. Tsipolitis

University of Ioánnina, Ioannina, Greece

I. Evangelou, C. Foudas, P. Giannelos, P. Katsoulis, P. Kokkas, S. Mallios, N. Manthos, I. Papadopoulos, E. Paradas, J. Strologas, F. A. Triantis, D. Tsitsonis

MTA-ELTE Lendület CMS Particle and Nuclear Physics Group, Eötvös Loránd University, Budapest, Hungary

M. Bartók²¹, M. Csanad, N. Filipovic, P. Major, M. I. Nagy, G. Pasztor, O. Surányi, G. I. Veres

Wigner Research Centre for Physics, Budapest, Hungary

G. Bencze, C. Hajdu, D. Horvath²², Á. Hunyadi, F. Sikler, T. Á. Vámi, V. Veszpremi, G. Vesztergombi[†]

Institute of Nuclear Research ATOMKI, Debrecen, Hungary

N. Beni, S. Czellar, J. Karancsi²³, A. Makovec, J. Molnar, Z. Szillasi

Institute of Physics, University of Debrecen, Debrecen, Hungary

P. Raics, Z. L. Trocsanyi, B. Ujvari

Indian Institute of Science (IISc), Bangalore, India

S. Choudhury, J. R. Komaragiri, P. C. Tiwari

National Institute of Science Education and Research, HBNI, Bhubaneswar, India

S. Bahinipati²⁴, C. Kar, P. Mal, K. Mandal, A. Nayak²⁵, D. K. Sahoo²⁴, S. K. Swain

Panjab University, Chandigarh, India

S. Bansal, S. B. Beri, V. Bhatnagar, S. Chauhan, R. Chawla, N. Dhingra, R. Gupta, A. Kaur, A. Kaur, M. Kaur, S. Kaur, R. Kumar, P. Kumari, M. Lohan, A. Mehta, K. Sandeep, S. Sharma, J. B. Singh, G. Walia

University of Delhi, Delhi, India

A. Bhardwaj, B. C. Choudhary, R. B. Garg, M. Gola, S. Keshri, Ashok Kumar, S. Malhotra, M. Naimuddin, P. Priyanka, K. Ranjan, Aashaq Shah, R. Sharma

Saha Institute of Nuclear Physics, HBNI, Kolkata, India

R. Bhardwaj²⁶, M. Bharti, R. Bhattacharya, S. Bhattacharya, U. Bhawandeep²⁶, D. Bhowmik, S. Dey, S. Dutt²⁶, S. Dutta, S. Ghosh, K. Mondal, S. Nandan, A. Purohit, P. K. Rout, A. Roy, S. Roy Chowdhury, S. Sarkar, M. Sharan, B. Singh, S. Thakur²⁶

Indian Institute of Technology Madras, Madras, India

P. K. Behera

Bhabha Atomic Research Centre, Mumbai, India

R. Chudasama, D. Dutta, V. Jha, V. Kumar, P. K. Netrakanti, L. M. Pant, P. Shukla

Tata Institute of Fundamental Research-A, Mumbai, India

T. Aziz, M. A. Bhat, S. Dugad, G. B. Mohanty, N. Sur, B. Sutar, RavindraKumar Verma

Tata Institute of Fundamental Research-B, Mumbai, India

S. Banerjee, S. Bhattacharya, S. Chatterjee, P. Das, M. Guchait, Sa. Jain, S. Karmakar, S. Kumar, M. Maity²⁷, G. Majumder, K. Mazumdar, N. Sahoo, T. Sarkar²⁷

Indian Institute of Science Education and Research (IISER), Pune, India

S. Chauhan, S. Dube, V. Hegde, A. Kapoor, K. Kothekar, S. Pandey, A. Rane, S. Sharma

Institute for Research in Fundamental Sciences (IPM), Tehran, Iran

S. Chenarani²⁸, E. Eskandari Tadavani, S. M. Etesami²⁸, M. Khakzad, M. Mohammadi Najafabadi, M. Naseri, F. Rezaei Hosseinabadi, B. Safarzadeh²⁹, M. Zeinali

University College Dublin, Dublin, Ireland

M. Felcini, M. Grunewald

INFN Sezione di Bari^a, Università di Bari^b, Politecnico di Bari^c, Bari, Italy

M. Abbrescia^{a,b}, C. Calabria^{a,b}, A. Colaleo^a, D. Creanza^{a,c}, L. Cristella^{a,b}, N. De Filippis^{a,c}, M. De Palma^{a,b}, A. Di Florio^{a,b}, F. Errico^{a,b}, L. Fiore^a, A. Gelmi^{a,b}, G. Iaselli^{a,c}, M. Ince^{a,b}, S. Lezki^{a,b}, G. Maggi^{a,c}, M. Maggi^a, G. Miniello^{a,b}, S. My^{a,b}, S. Nuzzo^{a,b}, A. Pompili^{a,b}, G. Pugliese^{a,c}, R. Radogna^a, A. Ranieri^a, G. Selvaggi^{a,b}, A. Sharma^a, L. Silvestris^a, R. Venditti^a, P. Verwilligen^a, G. Zito^a

INFN Sezione di Bologna^a, Università di Bologna^b, Bologna, Italy

G. Abbiendi^a, C. Battilana^{a,b}, D. Bonacorsi^{a,b}, L. Borgonovi^{a,b}, S. Braibant-Giacomelli^{a,b}, R. Campanini^{a,b}, P. Capiluppi^{a,b}, A. Castro^{a,b}, F. R. Cavallo^a, S. S. Chhibra^{a,b}, C. Ciocca^a, G. Codispoti^{a,b}, M. Cuffiani^{a,b}, G. M. Dallavalle^a, F. Fabbri^a, A. Fanfani^{a,b}, P. Giacomelli^a, C. Grandi^a, L. Guiducci^{a,b}, F. Iemmi^{a,b}, S. Marcellini^a, G. Masetti^a, A. Montanari^a, F. L. Navarria^{a,b}, A. Perrotta^a, F. Primavera^{a,b,17}, A. M. Rossi^{a,b}, T. Rovelli^{a,b}, G. P. Siroli^{a,b}, N. Tosi^a

INFN Sezione di Catania^a, Università di Catania^b, Catania, Italy

S. Albergo^{a,b}, A. Di Mattia^a, R. Potenza^{a,b}, A. Tricomi^{a,b}, C. Tuve^{a,b}

INFN Sezione di Firenze^a, Università di Firenze^b, Firenze, Italy

G. Barbagli^a, K. Chatterjee^{a,b}, V. Ciulli^{a,b}, C. Civinini^a, R. D'Alessandro^{a,b}, E. Focardi^{a,b}, G. Latino, P. Lenzi^{a,b}, M. Meschini^a, S. Paoletti^a, L. Russo^{a,30}, G. Sguazzoni^a, D. Strom^a, L. Viliani^a

INFN Laboratori Nazionali di Frascati, Frascati, Italy

L. Benussi, S. Bianco, F. Fabbri, D. Piccolo

INFN Sezione di Genova^a, Università di Genova^b, Genoa, Italy

F. Ferro^a, F. Ravera^{a,b}, E. Robutti^a, S. Tosi^{a,b}

INFN Sezione di Milano-Bicocca^a, Università di Milano-Bicocca^b, Milan, Italy

A. Benaglia^a, A. Beschi^b, L. Brianza^{a,b}, F. Brivio^{a,b}, V. Ciriolo^{a,b,17}, S. Di Guida^{a,d,17}, M. E. Dinardo^{a,b}, S. Fiorendi^{a,b}, S. Gennai^a, A. Ghezzi^{a,b}, P. Govoni^{a,b}, M. Malberti^{a,b}, S. Malvezzi^a, A. Massironi^{a,b}, D. Menasce^a, L. Moroni^a, M. Paganoni^{a,b}, D. Pedrini^a, S. Ragazzi^{a,b}, T. Tabarelli de Fatis^{a,b}

INFN Sezione di Napoli^a, Università di Napoli 'Federico II'^b, Naples, Italy, Università della Basilicata^c, Potenza, Italy, Università G. Marconi^d, Rome, Italy

S. Buontempo^a, N. Cavallo^{a,c}, A. Di Crescenzo^{a,b}, A. Di Crescenzo^{a,b}, F. Fabozzi^{a,c}, F. Fienga^a, G. Galati^a, A. O. M. Iorio^{a,b}, W. A. Khan^a, L. Lista^a, S. Meola^{a,d,17}, P. Paolucci^{a,17}, C. Sciacca^{a,b}, E. Voevodina^{a,b}

INFN Sezione di Padova^a, Università di Padova^b, Padova, Italy, Università di Trento^c, Trento, Italy

P. Azzi^a, N. Bacchetta^a, D. Bisello^{a,b}, A. Boletti^{a,b}, A. Bragagnolo, R. Carlin^{a,b}, P. Checchia^a, M. Dall'Osso^{a,b}, P. De Castro Manzano^a, T. Dorigo^a, U. Dosselli^a, F. Gasparini^{a,b}, U. Gasparini^{a,b}, A. Gozzelino^a, S. Lacaprara^a, P. Lujan, M. Margoni^{a,b}, A. T. Meneguzzo^{a,b}, J. Pazzini^{a,b}, P. Ronchese^{a,b}, R. Rossin^{a,b}, F. Simonetto^{a,b}, A. Tiko, E. Torassa^a, M. Zanetti^{a,b}, P. Zotto^{a,b}, G. Zumerle^{a,b}

INFN Sezione di Pavia^a, Università di Pavia^b, Pavia, Italy

A. Braghieri^a, A. Magnani^a, P. Montagna^{a,b}, S. P. Ratti^{a,b}, V. Re^a, M. Ressegotti^{a,b}, C. Riccardi^{a,b}, P. Salvini^a, I. Vai^{a,b}, P. Vitulo^{a,b}

INFN Sezione di Perugia^a, Università di Perugia^b, Perugia, Italy

L. Alunni Solestizi^{a,b}, M. Biasini^{a,b}, G. M. Bilei^a, C. Cecchi^{a,b}, D. Ciangottini^{a,b}, L. Fanò^{a,b}, P. Lariccia^{a,b}, R. Leonardi^{a,b}, E. Manoni^a, G. Mantovani^{a,b}, V. Mariani^{a,b}, M. Menichelli^a, A. Rossi^{a,b}, A. Santocchia^{a,b}, D. Spiga^a

INFN Sezione di Pisa^a, Università di Pisa^b, Scuola Normale Superiore di Pisa^c, Pisa, Italy

K. Androsov^a, P. Azzurri^a, G. Bagliesi^a, L. Bianchini^a, T. Boccali^a, L. Borrello, R. Castaldi^a, M. A. Ciocci^{a,b}, R. Dell'Orso^a, G. Fedì^a, F. Fiori^{a,c}, L. Giannini^{a,c}, A. Giassi^a, M. T. Grippo^a, F. Ligabue^{a,c}, E. Manca^{a,c}, G. Mandorli^{a,c}, A. Messineo^{a,b}, F. Palla^a, A. Rizzi^{a,b}, P. Spagnolo^a, R. Tenchini^a, G. Tonelli^{a,b}, A. Venturi^a, P. G. Verdini^a

INFN Sezione di Roma^a, Sapienza Università di Roma^b, Rome, Italy

L. Barone^{a,b}, F. Cavallari^a, M. Cipriani^{a,b}, N. Daci^a, D. Del Re^{a,b}, E. Di Marco^{a,b}, M. Diemoz^a, S. Gelli^{a,b}, E. Longo^{a,b}, B. Marzocchi^{a,b}, P. Meridiani^a, G. Organtini^{a,b}, F. Pandolfi^a, R. Paramatti^{a,b}, F. Preiato^{a,b}, S. Rahatlou^{a,b}, C. Rovelli^a, F. Santanastasio^{a,b}

INFN Sezione di Torino^a, Università di Torino^b, Torino, Italy, Università del Piemonte Orientale^c, Novara, Italy

N. Amapane^{a,b}, R. Arcidiacono^{a,c}, S. Argiro^{a,b}, M. Arneodo^{a,c}, N. Bartosik^a, R. Bellan^{a,b}, C. Biino^a, N. Cartiglia^a, F. Cenna^{a,b}, S. Cometti, M. Costa^{a,b}, R. Covarelli^{a,b}, N. Demaria^a, B. Kiani^{a,b}, C. Mariotti^a, S. Maselli^a, E. Migliore^{a,b}, V. Monaco^{a,b}, E. Monteil^{a,b}, M. Monteno^a, M. M. Obertino^{a,b}, L. Pacher^{a,b}, N. Pastrone^a, M. Pelliccioni^a, G. L. Pinna Angioni^{a,b}, A. Romero^{a,b}, M. Ruspa^{a,c}, R. Sacchi^{a,b}, K. Shchelina^{a,b}, V. Sola^a, A. Solano^{a,b}, D. Soldi, A. Staiano^a

INFN Sezione di Trieste^a, Università di Trieste^b, Trieste, Italy

S. Belforte^a, V. Candelise^{a,b}, M. Casarsa^a, F. Cossutti^a, G. Della Ricca^{a,b}, F. Vazzoler^{a,b}, A. Zanetti^a

Kyungpook National University, Daegu, Korea

D. H. Kim, G. N. Kim, M. S. Kim, J. Lee, S. Lee, S. W. Lee, C. S. Moon, Y. D. Oh, S. Sekmen, D. C. Son, Y. C. Yang

Chonnam National University, Institute for Universe and Elementary Particles, Kwangju, Korea

H. Kim, D. H. Moon, G. Oh

Hanyang University, Seoul, Korea

J. Goh³¹, T. J. Kim

Korea University, Seoul, Korea

S. Cho, S. Choi, Y. Go, D. Gyun, S. Ha, B. Hong, Y. Jo, K. Lee, K. S. Lee, S. Lee, J. Lim, S. K. Park, Y. Roh

Sejong University, Seoul, Korea

H. S. Kim

Seoul National University, Seoul, Korea

J. Almond, J. Kim, J. S. Kim, H. Lee, K. Lee, K. Nam, S. B. Oh, B. C. Radburn-Smith, S. h. Seo, U. K. Yang, H. D. Yoo, G. B. Yu

University of Seoul, Seoul, Korea

D. Jeon, H. Kim, J. H. Kim, J. S. H. Lee, I. C. Park

Sungkyunkwan University, Suwon, Korea

Y. Choi, C. Hwang, J. Lee, I. Yu

Vilnius University, Vilnius, Lithuania

V. Dudenias, A. Juodagalvis, J. Vaitkus

National Centre for Particle Physics, Universiti Malaya, Kuala Lumpur, Malaysia

I. Ahmed, Z. A. Ibrahim, M. A. B. Md Ali³², F. Mohamad Idris³³, W. A. T. Wan Abdullah, M. N. Yusli, Z. Zolkapli

Universidad de Sonora (UNISON), Hermosillo, Mexico

A. Castaneda Hernandez, J. A. Murillo Quijada

Centro de Investigacion y de Estudios Avanzados del IPN, Mexico City, Mexico

H. Castilla-Valdez, E. De La Cruz-Burelo, M. C. Duran-Osuna, I. Heredia-De La Cruz³⁴, R. Lopez-Fernandez, J. Mejia Guisao, R. I. Rabadan-Trejo, G. Ramirez-Sanchez, R. Reyes-Almanza, A. Sanchez-Hernandez

Universidad Iberoamericana, Mexico City, Mexico

S. Carrillo Moreno, C. Oropeza Barrera, F. Vazquez Valencia

Benemerita Universidad Autonoma de Puebla, Puebla, Mexico

J. Eysermans, I. Pedraza, H. A. Salazar Ibarguen, C. Uribe Estrada

Universidad Autónoma de San Luis Potosí, San Luis Potosí, Mexico

A. Morelos Pineda

University of Auckland, Auckland, New Zealand

D. Krofcheck

University of Canterbury, Christchurch, New Zealand

S. Bheesette, P. H. Butler

National Centre for Physics, Quaid-I-Azam University, Islamabad, Pakistan

A. Ahmad, M. Ahmad, M. I. Asghar, Q. Hassan, H. R. Hoorani, A. Saddique, M. A. Shah, M. Shoaib, M. Waqas

National Centre for Nuclear Research, Swierk, Poland

H. Bialkowska, M. Bluj, B. Boimska, T. Frueboes, M. Górski, M. Kazana, K. Nawrocki, M. Szleper, P. Traczyk, P. Zalewski

Institute of Experimental Physics, Faculty of Physics, University of Warsaw, Warsaw, Poland

K. Bunkowski, A. Byszuk³⁵, K. Doroba, A. Kalinowski, M. Konecki, J. Krolikowski, M. Misiura, M. Olszewski, A. Pyskir, M. Walczak

Laboratório de Instrumentação e Física Experimental de Partículas, Lisbon, Portugal

P. Bargassa, C. Beirão Da Cruz E Silva, A. Di Francesco, P. Faccioli, B. Galinhas, M. Gallinaro, J. Hollar, N. Leonardo, L. Lloret Iglesias, M. V. Nemallapudi, J. Seixas, G. Strong, O. Toldaiev, D. Vadrucio, J. Varela

Joint Institute for Nuclear Research, Dubna, Russia

P. Bunin, A. Golunov, I. Golutvin, V. Karjavin, V. Korenkov, G. Kozlov, A. Lanev, A. Malakhov, V. Matveev^{36,37}, V. V. Mitsyn, P. Moisezenz, V. Palichik, V. Perelygin, S. Shmatov, V. Smirnov, V. Trofimov, B. S. Yuldashev³⁸, A. Zarubin, V. Zhiltsov

Petersburg Nuclear Physics Institute, Gatchina (St. Petersburg), Russia

V. Golovtsov, Y. Ivanov, V. Kim³⁹, E. Kuznetsova⁴⁰, P. Levchenko, V. Murzin, V. Oreshkin, I. Smirnov, D. Sosnov, V. Sulimov, L. Uvarov, S. Vavilov, A. Vorobyev

Institute for Nuclear Research, Moscow, Russia

Yu. Andreev, A. Dermenev, S. Gninenko, N. Golubev, A. Karneyeu, M. Kirsanov, N. Krasnikov, A. Pashenkov, D. Tlisov, A. Toropin

Institute for Theoretical and Experimental Physics, Moscow, Russia

V. Epshteyn, V. Gavrilov, N. Lychkovskaya, V. Popov, I. Pozdnyakov, G. Safronov, A. Spiridonov, A. Stepenov, V. Stolin, M. Toms, E. Vlasov, A. Zhokin

Moscow Institute of Physics and Technology, Moscow, Russia

T. Aushev

National Research Nuclear University ‘Moscow Engineering Physics Institute’ (MEPhI), Moscow, Russia

M. Chadeeva⁴¹, P. Parygin, D. Philippov, S. Polikarpov⁴¹, E. Popova, V. Rusinov

P.N. Lebedev Physical Institute, Moscow, Russia

V. Andreev, M. Azarkin³⁷, I. Dremin³⁷, M. Kirakosyan³⁷, S. V. Rusakov, A. Terkulov

Skobeltsyn Institute of Nuclear Physics, Lomonosov Moscow State University, Moscow, Russia

A. Baskakov, A. Belyaev, E. Boos, A. Ershov, A. Gribushin, L. Khein, V. Klyukhin, O. Kodolova, I. Lokhtin, O. Lukina, I. Miagkov, S. Obraztsov, S. Petrushanko, V. Savrin, A. Snigirev

Novosibirsk State University (NSU), Novosibirsk, Russia

V. Blinov⁴², T. Dimova⁴², L. Kardapol'tsev⁴², D. Shtol⁴², Y. Skovpen⁴²

Institute for High Energy Physics of National Research Centre 'Kurchatov Institute', Protvino, Russia

I. Azhgirey, I. Bayshev, S. Bitioukov, D. Elumakhov, A. Godizov, V. Kachanov, A. Kalinin, D. Konstantinov, P. Mandrik, V. Petrov, R. Ryutin, S. Slabospitskii, A. Sobol, S. Troshin, N. Tyurin, A. Uzunian, A. Volkov

National Research Tomsk Polytechnic University, Tomsk, Russia

A. Babaev, S. Baidali

University of Belgrade, Faculty of Physics and Vinca Institute of Nuclear Sciences, Belgrade, Serbia

P. Adzic⁴³, P. Cirkovic, D. Devetak, M. Dordevic, J. Milosevic

Centro de Investigaciones Energéticas Medioambientales y Tecnológicas (CIEMAT), Madrid, Spain

J. Alcaraz Maestre, A. Álvarez Fernández, I. Bachiller, M. Barrio Luna, J. A. Brochero Cifuentes, M. Cerrada, N. Colino, B. De La Cruz, A. Delgado Peris, C. Fernandez Bedoya, J. P. Fernández Ramos, J. Flix, M. C. Fouz, O. Gonzalez Lopez, S. Goy Lopez, J. M. Hernandez, M. I. Josa, D. Moran, A. Pérez-Calero Yzquierdo, J. Puerta Pelayo, I. Redondo, L. Romero, M. S. Soares, A. Triossi

Universidad Autónoma de Madrid, Madrid, Spain

C. Albajar, J. F. de Trocóniz

Universidad de Oviedo, Oviedo, Spain

J. Cuevas, C. Erice, J. Fernandez Menendez, S. Folgueras, I. Gonzalez Caballero, J. R. González Fernández, E. Palencia Cortezon, V. Rodríguez Bouza, S. Sanchez Cruz, P. Vischia, J. M. Vizán García

Instituto de Física de Cantabria (IFCA), CSIC-Universidad de Cantabria, Santander, Spain

I. J. Cabrillo, A. Calderon, B. Chazin Quero, J. Duarte Campderros, M. Fernandez, P. J. Fernández Manteca, A. García Alonso, J. Garcia-Ferrero, G. Gomez, A. Lopez Virto, J. Marco, C. Martinez Rivero, P. Martinez Ruiz del Arbol, F. Matorras, J. Piedra Gomez, C. Prieels, T. Rodrigo, A. Ruiz-Jimeno, L. Scodellaro, N. Trevisani, I. Vila, R. Vilar Cortabitarte

CERN, European Organization for Nuclear Research, Geneva, Switzerland

D. Abbaneo, B. Akgun, E. Auffray, P. Baillon, A. H. Ball, D. Barney, J. Bendavid, M. Bianco, A. Bocci, C. Botta, E. Brondolin, T. Camporesi, M. Cepeda, G. Cerminara, E. Chapon, Y. Chen, G. Cucciati, D. d'Enterria, A. Dabrowski, V. Daponte, A. David, A. De Roeck, N. Deelen, M. Dobson, T. du Pree, M. Dünser, N. Dupont, A. Elliott-Peisert, P. Everaerts, F. Fallavollita⁴⁴, D. Fasanella, G. Franzoni, J. Fulcher, W. Funk, D. Gigi, A. Gilbert, K. Gill, F. Glege, M. Guilbaud, D. Gulhan, J. Hegeman, V. Innocente, A. Jafari, P. Janot, O. Karacheban²⁰, J. Kieseler, A. Kornmayer, M. Krammer¹, C. Lange, P. Lecoq, C. Lourenço, L. Malgeri, M. Mannelli, F. Meijers, J. A. Merlin, S. Mersi, E. Meschi, P. Milenovic⁴⁵, F. Moortgat, M. Mulders, J. Ngadiuba, S. Orfanelli, L. Orsini, F. Pantaleo¹⁷, L. Pape, E. Perez, M. Peruzzi, A. Petrilli, G. Petrucciani, A. Pfeiffer, M. Pierini, F. M. Pitters, D. Rabady, A. Racz, T. Reis, G. Rolandi⁴⁶, M. Rovere, H. Sakulin, C. Schäfer, C. Schwick, M. Seidel, M. Selvaggi, A. Sharma, P. Silva, P. Sphicas⁴⁷, A. Stakia, J. Steggemann, M. Tosi, D. Treille, A. Tsirou, V. Veckalns⁴⁸, W. D. Zeuner

Paul Scherrer Institut, Villigen, Switzerland

L. Caminada⁴⁹, K. Deiters, W. Erdmann, R. Horisberger, Q. Ingram, H. C. Kaestli, D. Kotlinski, U. Langenegger, T. Rohe, S. A. Wiederkehr

ETH Zurich - Institute for Particle Physics and Astrophysics (IPA), Zurich, Switzerland

M. Backhaus, L. Bäni, P. Berger, N. Chernyavskaya, G. Dissertori, M. Dittmar, M. Donegà, C. Dorfer, C. Grab, C. Heidegger, D. Hits, J. Hoss, T. Klijnsmas, W. Lustermaan, R. A. Manzoni, M. Marionneau, M. T. Meinhard, F. Micheli, P. Musella, F. Nessi-Tedaldi, J. Pata, F. Pauss, G. Perrin, L. Perrozzi, S. Pigazzini, M. Quittnat, D. Ruini, D. A. Sanz Becerra, M. Schönenberger, L. Shchutska, V. R. Tavolaro, K. Theofilatos, M. L. Vesterbacka Olsson, R. Wallny, D. H. Zhu

Universität Zürich, Zurich, Switzerland

T. K. Aarrestad, C. Amsler⁵⁰, D. Brzhechko, M. F. Canelli, A. De Cosa, R. Del Burgo, S. Donato, C. Galloni, T. Hreus, B. Kilminster, I. Neutelings, D. Pinna, G. Rauco, P. Robmann, D. Salerno, K. Schweiger, C. Seitz, Y. Takahashi, A. Zucchetta

National Central University, Chung-Li, Taiwan

Y. H. Chang, K. y. Cheng, T. H. Doan, Sh. Jain, R. Khurana, C. M. Kuo, W. Lin, A. Pozdnyakov, S. S. Yu

National Taiwan University (NTU), Taipei, Taiwan

P. Chang, Y. Chao, K. F. Chen, P. H. Chen, W.-S. Hou, Arun Kumar, Y. y. Li, Y. F. Liu, R.-S. Lu, E. Paganis, A. Psallidas, A. Steen, J. f. Tsai

Chulalongkorn University, Faculty of Science, Department of Physics, Bangkok, Thailand

B. Asavapibhop, N. Srimanobhas, N. Suwonjandee

Çukurova University, Physics Department, Science and Art Faculty, Adana, Turkey

A. Bat, F. Boran, S. Cerci⁵¹, S. Damarseckin, Z. S. Demiroglu, F. Dolek, C. Dozen, E. Eskut, S. Girgis, G. Gokbulut, Y. Guler, E. Gurpinar, I. Hos⁵², C. Isik, E. E. Kangal⁵³, O. Kara, U. Kiminsu, M. Oglakci, G. Onengut, K. Ozdemir⁵⁴, S. Ozturk⁵⁵, A. Polatoz, D. Sunar Cerci⁵¹, U. G. Tok, H. Topakli⁵⁵, S. Turccapar, I. S. Zorbakir, C. Zorbilmez

Middle East Technical University, Physics Department, Ankara, Turkey

B. Isildak⁵⁶, G. Karapinar⁵⁷, M. Yalvac, M. Zeyrek

Bogazici University, Istanbul, Turkey

I. O. Atakisi, E. Gülmez, M. Kaya⁵⁸, O. Kaya⁵⁹, S. Ozkorucuklu⁶⁰, S. Tekten, E. A. Yetkin⁶¹

Istanbul Technical University, Istanbul, Turkey

M. N. Agaras, S. Atay, A. Cakir, K. Cankocak, Y. Komurcu, S. Sen⁶²

Institute for Scintillation Materials of National Academy of Science of Ukraine, Kharkov, Ukraine

B. Grynyov

National Scientific Center, Kharkov Institute of Physics and Technology, Kharkov, Ukraine

L. Levchuk

University of Bristol, Bristol, UK

F. Ball, L. Beck, J. J. Brooke, D. Burns, E. Clement, D. Cussans, O. Davignon, H. Flacher, J. Goldstein, G. P. Heath, H. F. Heath, L. Kreczko, D. M. Newbold⁶³, S. Paramesvaran, B. Penning, T. Sakuma, D. Smith, V. J. Smith, J. Taylor, A. Titterton

Rutherford Appleton Laboratory, Didcot, UK

K. W. Bell, A. Belyaev⁶⁴, C. Brew, R. M. Brown, D. Cieri, D. J. A. Cockerill, J. A. Coughlan, K. Harder, S. Harper, J. Linacre, E. Olaiya, D. Petyt, C. H. Shepherd-Themistocleous, A. Thea, I. R. Tomalin, T. Williams, W. J. Womersley

Imperial College, London, UK

G. Auzinger, R. Bainbridge, P. Bloch, J. Borg, S. Breeze, O. Buchmuller, A. Bundock, S. Casasso, D. Colling, L. Corpe, P. Dauncey, G. Davies, M. Della Negra, R. Di Maria, Y. Haddad, G. Hall, G. Iles, T. James, M. Komm, C. Laner, L. Lyons, A.-M. Magnan, S. Malik, A. Martelli, J. Nash⁶⁵, A. Nikitenko⁷, V. Palladino, M. Pesaresi, A. Richards, A. Rose, E. Scott, C. Seez, A. Shtipliyski, G. Singh, M. Stoye, T. Strebler, S. Summers, A. Tapper, K. Uchida, T. Virdee¹⁷, N. Wardle, D. Winterbottom, J. Wright, S. C. Zenz

Brunel University, Uxbridge, UK

J. E. Cole, P. R. Hobson, A. Khan, P. Kyberd, C. K. Mackay, A. Morton, I. D. Reid, L. Teodorescu, S. Zahid

Baylor University, Waco, USA

K. Call, J. Dittmann, K. Hatakeyama, H. Liu, C. Madrid, B. McMaster, N. Pastika, C. Smith

Catholic University of America, Washington, DC, USA

R. Bartek, A. Dominguez

The University of Alabama, Tuscaloosa, USA

A. Buccilli, S. I. Cooper, C. Henderson, P. Rumerio, C. West

Boston University, Boston, USA

D. Arcaro, T. Bose, D. Gastler, D. Rankin, C. Richardson, J. Rohlf, L. Sulak, D. Zou

Brown University, Providence, USA

G. Benelli, X. Coubez, D. Cutts, M. Hadley, J. Hakala, U. Heintz, J. M. Hogan⁶⁶, K. H. M. Kwok, E. Laird, G. Landsberg, J. Lee, Z. Mao, M. Narain, S. Piperov, S. Sagir⁶⁷, R. Syarif, E. Usai, D. Yu

University of California, Davis, Davis, USA

R. Band, C. Brainerd, R. Breedon, D. Burns, M. Calderon De La Barca Sanchez, M. Chertok, J. Conway, R. Conway, P. T. Cox, R. Erbacher, C. Flores, G. Funk, W. Ko, O. Kukral, R. Lander, C. Mclean, M. Mulhearn, D. Pellett, J. Pilot, S. Shalhout, M. Shi, D. Stolp, D. Taylor, K. Tos, M. Tripathi, Z. Wang, F. Zhang

University of California, Los Angeles, USA

M. Bachtis, C. Bravo, R. Cousins, A. Dasgupta, A. Florent, J. Hauser, M. Ignatenko, N. Mccoll, S. Regnard, D. Saltzberg, C. Schnaible, V. Valuev

University of California, Riverside, Riverside, USA

E. Bouvier, K. Burt, R. Clare, J. W. Gary, S. M. A. Ghiasi Shirazi, G. Hanson, G. Karapostoli, E. Kennedy, F. Lacroix, O. R. Long, M. Olmedo Negrete, M. I. Paneva, W. Si, L. Wang, H. Wei, S. Wimpenny, B. R. Yates

University of California, San Diego, La Jolla, USA

J. G. Branson, S. Cittolin, M. Derdzinski, R. Gerosa, D. Gilbert, B. Hashemi, A. Holzner, D. Klein, G. Kole, V. Krutelyov, J. Letts, M. Masciovecchio, D. Olivito, S. Padhi, M. Pieri, M. Sani, V. Sharma, S. Simon, M. Tadel, A. Vartak, S. Wasserbaech⁶⁸, J. Wood, F. Würthwein, A. Yagil, G. Zevi Della Porta

University of California, Santa Barbara - Department of Physics, Santa Barbara, USA

N. Amin, R. Bhandari, J. Bradmiller-Feld, C. Campagnari, M. Citron, A. Dishaw, V. Dutta, M. Franco Sevilla, L. Gouskos, R. Heller, J. Incandela, A. Ovcharova, H. Qu, J. Richman, D. Stuart, I. Suarez, S. Wang, J. Yoo

California Institute of Technology, Pasadena, USA

D. Anderson, A. Bornheim, J. M. Lawhorn, H. B. Newman, T. Q. Nguyen, M. Spiropulu, J. R. Vlimant, R. Wilkinson, S. Xie, Z. Zhang, R. Y. Zhu

Carnegie Mellon University, Pittsburgh, USA

M. B. Andrews, T. Ferguson, T. Mudholkar, M. Paulini, M. Sun, I. Vorobiev, M. Weinberg

University of Colorado Boulder, Boulder, USA

J. P. Cumalat, W. T. Ford, F. Jensen, A. Johnson, M. Krohn, S. Leontsinis, E. MacDonald, T. Mulholland, K. Stenson, K. A. Ulmer, S. R. Wagner

Cornell University, Ithaca, USA

J. Alexander, J. Chaves, Y. Cheng, J. Chu, A. Datta, K. McDermott, N. Mirman, J. R. Patterson, D. Quach, A. Rinkevicius, A. Ryd, L. Skinnari, L. Soffi, S. M. Tan, Z. Tao, J. Thom, J. Tucker, P. Wittich, M. Zientek

Fermi National Accelerator Laboratory, Batavia, USA

S. Abdullin, M. Albrow, M. Alyari, G. Apollinari, A. Apresyan, A. Apyan, S. Banerjee, L. A. T. Bauerick, A. Beretvas, J. Berryhill, P. C. Bhat, G. Bolla[†], K. Burkett, J. N. Butler, A. Canepa, G. B. Cerati, H. W. K. Cheung, F. Chlebana, M. Cremonesi, J. Duarte, V. D. Elvira, J. Freeman, Z. Gecse, E. Gottschalk, L. Gray, D. Green, S. Grünendahl, O. Gutsche, J. Hanlon, R. M. Harris, S. Hasegawa, J. Hirschauer, Z. Hu, B. Jayatilaka, S. Jindariani, M. Johnson, U. Joshi, B. Klima, M. J. Kortelainen, B. Kreis, S. Lammel, D. Lincoln, R. Lipton, M. Liu, T. Liu, J. Lykken, K. Maeshima, J. M. Marraffino, D. Mason, P. McBride, P. Merkel, S. Mrenna, S. Nahn, V. O'Dell, K. Pedro, C. Pena, O. Prokofyev, G. Rakness, L. Ristori, A. Savoy-Navarro⁶⁹, B. Schneider, E. Sexton-Kennedy, A. Soha, W. J. Spalding, L. Spiegel, S. Stoynev, J. Strait, N. Strobbe, L. Taylor, S. Tkaczyk, N. V. Tran, L. Uplegger, E. W. Vaandering, C. Vernieri, M. Verzocchi, R. Vidal, M. Wang, H. A. Weber, A. Whitbeck

University of Florida, Gainesville, USA

D. Acosta, P. Avery, P. Bortignon, D. Bourilkov, A. Brinkerhoff, L. Cadamuro, A. Carnes, M. Carver, D. Curry, R. D. Field, S. V. Gleyzer, B. M. Joshi, J. Konigsberg, A. Korytov, P. Ma, K. Matchev, H. Mei, G. Mitselmakher, K. Shi, D. Sperka, J. Wang, S. Wang

Florida International University, Miami, USA

Y. R. Joshi, S. Linn

Florida State University, Tallahassee, USA

A. Ackert, T. Adams, A. Askew, S. Hagopian, V. Hagopian, K. F. Johnson, T. Kolberg, G. Martinez, T. Perry, H. Prosper, A. Saha, V. Sharma, R. Yohay

Florida Institute of Technology, Melbourne, USA

M. M. Baarmand, V. Bhopatkar, S. Colafranceschi, M. Hohlmann, D. Noonan, M. Rahmani, T. Roy, F. Yumiceva

University of Illinois at Chicago (UIC), Chicago, USA

M. R. Adams, L. Apanasevich, D. Berry, R. R. Betts, R. Cavanaugh, X. Chen, S. Dittmer, O. Evdokimov, C. E. Gerber, D. A. Hangal, D. J. Hofman, K. Jung, J. Kamin, C. Mills, I. D. Sandoval Gonzalez, M. B. Tonjes, N. Varelas, H. Wang, X. Wang, Z. Wu, J. Zhang

The University of Iowa, Iowa City, USA

M. Alhusseini, B. Bilki⁷⁰, W. Clarida, K. Dilsiz⁷¹, S. Durgut, R. P. Gandrajula, M. Haytmyradov, V. Khristenko, J.-P. Merlo, A. Mestvirishvili, A. Moeller, J. Nachtman, H. Ogul⁷², Y. Onel, F. Ozok⁷³, A. Penzo, C. Snyder, E. Tiras, J. Wetzel

Johns Hopkins University, Baltimore, USA

B. Blumenfeld, A. Cocoros, N. Eminizer, D. Fehling, L. Feng, A. V. Gritsan, W. T. Hung, P. Maksimovic, J. Roskes, U. Sarica, M. Swartz, M. Xiao, C. You

The University of Kansas, Lawrence, USA

A. Al-bataineh, P. Baringer, A. Bean, S. Boren, J. Bowen, A. Bylinkin, J. Castle, S. Khalil, A. Kropivnitskaya, D. Majumder, W. Mcbrayer, M. Murray, C. Rogan, S. Sanders, E. Schmitz, J. D. Tapia Takaki, Q. Wang

Kansas State University, Manhattan, USA

S. Duric, A. Ivanov, K. Kaadze, D. Kim, Y. Maravin, D. R. Mendis, T. Mitchell, A. Modak, A. Mohammadi, L. K. Saini, N. Skhirtladze

Lawrence Livermore National Laboratory, Livermore, USA

F. Rebassoo, D. Wright

University of Maryland, College Park, USA

A. Baden, O. Baron, A. Belloni, S. C. Eno, Y. Feng, C. Ferraioli, N. J. Hadley, S. Jabeen, G. Y. Jeng, R. G. Kellogg, J. Kunkle, A. C. Mignerey, F. Ricci-Tam, Y. H. Shin, A. Skuja, S. C. Tonwar, K. Wong

Massachusetts Institute of Technology, Cambridge, USA

D. Abercrombie, B. Allen, V. Azzolini, A. Baty, G. Bauer, R. Bi, S. Brandt, W. Busza, I. A. Cali, M. D'Alfonso, Z. Demiragli, G. Gomez Ceballos, M. Goncharov, P. Harris, D. Hsu, M. Hu, Y. Iiyama, G. M. Innocenti, M. Klute, D. Kovalskyi, Y.-J. Lee, P. D. Luckey, B. Maier, A. C. Marini, C. McGinn, C. Mironov, S. Narayanan, X. Niu, C. Paus,

C. Roland, G. Roland, G. S. F. Stephans, K. Sumorok, K. Tatar, D. Velicanu, J. Wang, T. W. Wang, B. Wyslouch, S. Zhaozhong

University of Minnesota, Minneapolis, USA

A. C. Benvenuti, R. M. Chatterjee, A. Evans, P. Hansen, S. Kalafut, Y. Kubota, Z. Lesko, J. Mans, S. Nourbakhsh, N. Ruckstuhl, R. Rusack, J. Turkewitz, M. A. Wadud

University of Mississippi, Oxford, USA

J. G. Acosta, S. Oliveros

University of Nebraska-Lincoln, Lincoln, USA

E. Avdeeva, K. Bloom, D. R. Claes, C. Fangmeier, F. Golf, R. Gonzalez Suarez, R. Kamalieddin, I. Kravchenko, J. Monroy, J. E. Siado, G. R. Snow, B. Stieger

State University of New York at Buffalo, Buffalo, USA

A. Godshalk, C. Harrington, I. Iashvili, A. Kharchilava, D. Nguyen, A. Parker, S. Rappoccio, B. Roozbahani

Northeastern University, Boston, USA

G. Alverson, E. Barberis, C. Freer, A. Hortiangtham, D. M. Morse, T. Orimoto, R. Teixeira De Lima, T. Wamorkar, B. Wang, A. Wisecarver, D. Wood

Northwestern University, Evanston, USA

S. Bhattacharya, O. Charaf, K. A. Hahn, N. Mucia, N. Odell, M. H. Schmitt, K. Sung, M. Trovato, M. Velasco

University of Notre Dame, Notre Dame, USA

R. Bucci, N. Dev, M. Hildreth, K. Hurtado Anampa, C. Jessop, D. J. Karmgard, N. Kellams, K. Lannon, W. Li, N. Loukas, N. Marinelli, F. Meng, C. Mueller, Y. Musienko³⁶, M. Planer, A. Reinsvold, R. Ruchti, P. Siddireddy, G. Smith, S. Taroni, M. Wayne, A. Wightman, M. Wolf, A. Woodard

The Ohio State University, Columbus, USA

J. Alimena, L. Antonelli, B. Bylsma, L. S. Durkin, S. Flowers, B. Francis, A. Hart, C. Hill, W. Ji, T. Y. Ling, W. Luo, B. L. Winer, H. W. Wulsin

Princeton University, Princeton, USA

S. Cooperstein, P. Elmer, J. Hardenbrook, P. Hebda, S. Higginbotham, A. Kalogeropoulos, D. Lange, M. T. Lucchini, J. Luo, D. Marlow, K. Mei, I. Ojalvo, J. Olsen, C. Palmer, P. Piroué, J. Salfeld-Nebgen, D. Stickland, C. Tully

University of Puerto Rico, Mayaguez, USA

S. Malik, S. Norberg

Purdue University, West Lafayette, USA

A. Barker, V. E. Barnes, S. Das, L. Gutay, M. Jones, A. W. Jung, A. Khatiwada, B. Mahakud, D. H. Miller, N. Neumeister, C. C. Peng, H. Qiu, J. F. Schulte, J. Sun, F. Wang, R. Xiao, W. Xie

Purdue University Northwest, Hammond, USA

T. Cheng, J. Dolen, N. Parashar

Rice University, Houston, USA

Z. Chen, K. M. Ecklund, S. Freed, F. J. M. Geurts, M. Kilpatrick, W. Li, B. Michlin, B. P. Padley, J. Roberts, J. Rorie, W. Shi, Z. Tu, J. Zabel, A. Zhang

University of Rochester, Rochester, USA

A. Bodek, P. de Barbaro, R. Demina, Y. t. Duh, J. L. Dulemba, C. Fallon, T. Ferbel, M. Galanti, A. Garcia-Bellido, J. Han, O. Hindrichs, A. Khukhunaishvili, K. H. Lo, P. Tan, R. Taus, M. Verzetti

The Rockefeller University, New York, USA

R. Ciesielski

Rutgers, The State University of New Jersey, Piscataway, USA

A. Agapitos, J. P. Chou, Y. Gershtein, T. A. Gómez Espinosa, E. Halkiadakis, M. Heindl, E. Hughes, S. Kaplan,

R. Kunnawalkam Elayavalli, S. Kyriacou, A. Lath, R. Montalvo, K. Nash, M. Osherson, H. Saka, S. Salur, S. Schnetzer, D. Sheffield, S. Somalwar, R. Stone, S. Thomas, P. Thomassen, M. Walker

University of Tennessee, Knoxville, USA

A. G. Delannoy, J. Heideman, G. Riley, K. Rose, S. Spanier, K. Thapa

Texas A & M University, College Station, USA

O. Bouhali⁷⁴, A. Celik, M. Dalchenko, M. De Mattia, A. Delgado, S. Dildick, R. Eusebi, J. Gilmore, T. Huang, T. Kamon⁷⁵, S. Luo, R. Mueller, Y. Pakhotin, R. Patel, A. Perloff, L. Perniè, D. Rathjens, A. Safonov, A. Tatarinov

Texas Tech University, Lubbock, USA

N. Akchurin, J. Damgov, F. De Guio, P. R. Duerdo, S. Kunori, K. Lamichhane, S. W. Lee, T. Mengke, S. Muthumuni, T. Peltola, S. Undleeb, I. Volobouev, Z. Wang

Vanderbilt University, Nashville, USA

S. Greene, A. Gurrola, R. Janjam, W. Johns, C. Maguire, A. Melo, H. Ni, K. Padeken, J. D. Ruiz Alvarez, P. Sheldon, S. Tuo, J. Velkovska, M. Verweij, Q. Xu

University of Virginia, Charlottesville, USA

M. W. Arenton, P. Barria, B. Cox, R. Hirosky, M. Joyce, A. Ledovskoy, H. Li, C. Neu, T. Sinthuprasith, Y. Wang, E. Wolfe, F. Xia

Wayne State University, Detroit, USA

R. Harr, P. E. Karchin, N. Poudyal, J. Sturdy, P. Thapa, S. Zaleski

University of Wisconsin-Madison, Madison, WI, USA

M. Brodski, J. Buchanan, C. Caillol, D. Carlsmith, S. Dasu, L. Dodd, B. Gomber, M. Grothe, M. Herndon, A. Hervé, U. Hussain, P. Klabbers, A. Lanaro, A. Levine, K. Long, R. Loveless, T. Ruggles, A. Savin, N. Smith, W. H. Smith, N. Woods

† Deceased

- 1: Also at Vienna University of Technology, Vienna, Austria
- 2: Also at IRFU, CEA, Université Paris-Saclay, Gif-sur-Yvette, France
- 3: Also at Universidade Estadual de Campinas, Campinas, Brazil
- 4: Also at Federal University of Rio Grande do Sul, Porto Alegre, Brazil
- 5: Also at Université Libre de Bruxelles, Brussels, Belgium
- 6: Also at University of Chinese Academy of Sciences, Beijing, China
- 7: Also at Institute for Theoretical and Experimental Physics, Moscow, Russia
- 8: Also at Joint Institute for Nuclear Research, Dubna, Russia
- 9: Now at Cairo University, Cairo, Egypt
- 10: Also at Fayoum University, El-Fayoum, Egypt
- 11: Now at British University in Egypt, Cairo, Egypt
- 12: Now at Ain Shams University, Cairo, Egypt
- 13: Also at Department of Physics, King Abdulaziz University, Jeddah, Saudi Arabia
- 14: Also at Université de Haute Alsace, Mulhouse, France
- 15: Also at Skobeltsyn Institute of Nuclear Physics, Lomonosov Moscow State University, Moscow, Russia
- 16: Also at Ilia State University, Tbilisi, Georgia
- 17: Also at CERN, European Organization for Nuclear Research, Geneva, Switzerland
- 18: Also at RWTH Aachen University, III. Physikalisches Institut A, Aachen, Germany
- 19: Also at University of Hamburg, Hamburg, Germany
- 20: Also at Brandenburg University of Technology, Cottbus, Germany
- 21: Also at MTA-ELTE Lendület CMS Particle and Nuclear Physics Group, Eötvös Loránd University, Budapest, Hungary
- 22: Also at Institute of Nuclear Research ATOMKI, Debrecen, Hungary
- 23: Also at Institute of Physics, University of Debrecen, Debrecen, Hungary
- 24: Also at Indian Institute of Technology Bhubaneswar, Bhubaneswar, India
- 25: Also at Institute of Physics, Bhubaneswar, India

- 26: Also at Shoolini University, Solan, India
- 27: Also at University of Visva-Bharati, Santiniketan, India
- 28: Also at Isfahan University of Technology, Isfahan, Iran
- 29: Also at Plasma Physics Research Center, Science and Research Branch, Islamic Azad University, Tehran, Iran
- 30: Also at Università degli Studi di Siena, Siena, Italy
- 31: Also at Kyung Hee University, Department of Physics, Seoul, Korea
- 32: Also at International Islamic University of Malaysia, Kuala Lumpur, Malaysia
- 33: Also at Malaysian Nuclear Agency, MOSTI, Kajang, Malaysia
- 34: Also at Consejo Nacional de Ciencia y Tecnología, Mexico City, Mexico
- 35: Also at Warsaw University of Technology, Institute of Electronic Systems, Warsaw, Poland
- 36: Also at Institute for Nuclear Research, Moscow, Russia
- 37: Now at National Research Nuclear University 'Moscow Engineering Physics Institute' (MEPhI), Moscow, Russia
- 38: Also at Institute of Nuclear Physics of the Uzbekistan Academy of Sciences, Tashkent, Uzbekistan
- 39: Also at St. Petersburg State Polytechnical University, St. Petersburg, Russia
- 40: Also at University of Florida, Gainesville, USA
- 41: Also at P.N. Lebedev Physical Institute, Moscow, Russia
- 42: Also at Budker Institute of Nuclear Physics, Novosibirsk, Russia
- 43: Also at Faculty of Physics, University of Belgrade, Belgrade, Serbia
- 44: Also at INFN Sezione di Pavia^a, Università di Pavia^b, Pavia, Italy
- 45: Also at University of Belgrade, Faculty of Physics and Vinca Institute of Nuclear Sciences, Belgrade, Serbia
- 46: Also at Scuola Normale e Sezione dell'INFN, Pisa, Italy
- 47: Also at National and Kapodistrian University of Athens, Athens, Greece
- 48: Also at Riga Technical University, Riga, Latvia
- 49: Also at Universität Zürich, Zurich, Switzerland
- 50: Also at Stefan Meyer Institute for Subatomic Physics (SMI), Vienna, Austria
- 51: Also at Adiyaman University, Adiyaman, Turkey
- 52: Also at Istanbul Aydin University, Istanbul, Turkey
- 53: Also at Mersin University, Mersin, Turkey
- 54: Also at Piri Reis University, Istanbul, Turkey
- 55: Also at Gaziosmanpasa University, Tokat, Turkey
- 56: Also at Ozyegin University, Istanbul, Turkey
- 57: Also at Izmir Institute of Technology, Izmir, Turkey
- 58: Also at Marmara University, Istanbul, Turkey
- 59: Also at Kafkas University, Kars, Turkey
- 60: Also at Istanbul University, Faculty of Science, Istanbul, Turkey
- 61: Also at Istanbul Bilgi University, Istanbul, Turkey
- 62: Also at Hacettepe University, Ankara, Turkey
- 63: Also at Rutherford Appleton Laboratory, Didcot, UK
- 64: Also at School of Physics and Astronomy, University of Southampton, Southampton, UK
- 65: Also at Monash University, Faculty of Science, Clayton, Australia
- 66: Also at Bethel University, St. Paul, USA
- 67: Also at Karamanoğlu Mehmetbey University, Karaman, Turkey
- 68: Also at Utah Valley University, Orem, USA
- 69: Also at Purdue University, West Lafayette, USA
- 70: Also at Beykent University, Istanbul, Turkey
- 71: Also at Bingol University, Bingol, Turkey
- 72: Also at Sinop University, Sinop, Turkey
- 73: Also at Mimar Sinan University, Istanbul, Istanbul, Turkey
- 74: Also at Texas A&M University at Qatar, Doha, Qatar
- 75: Also at Kyungpook National University, Daegu, Korea